

Food and Chemical Toxicology

Inhibition of activity/expression, or genetic deletion, of ERO1 α blunts arsenite geno- and cyto-toxicity

--Manuscript Draft--

Manuscript Number:	FCT-D-22-01057R2
Article Type:	Full Length Article
Keywords:	Arsenite; ERO1 α ; mitochondrial Ca ²⁺ ; mitochondrial superoxide; DNA damage; Apoptosis
Corresponding Author:	Orazio Cantoni University of Urbino, Italy Urbino, ITALY
First Author:	Andrea Guidarelli
Order of Authors:	Andrea Guidarelli Andrea Spina Mara Fiorani Ester Zito Orazio Cantoni
Abstract:	<p>Our recent studies suggest that arsenite stimulates the crosstalk between the inositol 1,4,5-triphosphate receptor and the ryanodine receptor (RyR) via a mechanism dependent on endoplasmic reticulum (ER) oxidoreductin1a (ERO1a) up-regulation. Under these conditions, the fraction of Ca²⁺ released by the RyR via an ERO1a-dependent mechanism was promptly cleared by the mitochondria and critically mediated O₂⁻ formation, responsible for the triggering of time-dependent events associated with strand scission of genomic DNA and delayed mitochondrial apoptosis. We herein report that, in differentiated C2C12 cells, this sequence of events can be intercepted by genetic deletion of ERO1a as well as by EN460, an inhibitor of ERO1a activity. Similar results were obtained for the early effects mediated by arsenite in proliferating U937 cells, in which however the long-term studies were hampered by the inhibitor intrinsic toxicity. It was then interesting to observe that ISRIB, an inhibitor of p-eIF2α, was in both cell types devoid of intrinsic toxicity and able to suppress ERO1a expression and the resulting downstream effects leading to arsenite geno- and cyto-toxicity. We therefore conclude that pharmacological inhibition of ERO1a activity, or expression, effectively counteracts the deleterious effects induced by the metalloid via a mechanism associated with prevention of mitochondrial O₂⁻ formation.</p>
Response to Reviewers:	<p>Response to reviewers' queries</p> <p>Reviewer 1</p> <ol style="list-style-type: none">1. Similarity index was high only in two sections of our first submission, References and Material and Methods. We cannot change the references. We instead introduced several changes in the Material and Methods section.2. Title was changed.3. New Western blots are presented in the revised version of the paper. Hope this reviewer find the acceptable in high resolution.4. We tried to improve the quality of writing.5. Title of Fig. 5 was changed. <p>Reviewer 2</p> <ol style="list-style-type: none">1. The experimental results illustrated in Fig. 3 indicate that treatment for up to 24 h with 10 μM EN460 is not toxic for WT D-C2C12, as measured by counting the number of trypan blue positive and negative cells, as well as the number of Hoechst positive cells. However, under identical conditions, EN460 failed to promote toxicity only at 6h, with a time-dependent induction of both necrotic (increase in trypan positive cells) and apoptotic death (increase in Hoechst positive cells) at 16 and 24 h. ISRIB (200 nM) instead failed to induce toxicity in both cell lines, under all of these conditions. The above experiments were therefore performed to select appropriate conditions to test the effect of ISRIB and EN460 on various toxicity endpoints induced by arsenite. These inhibitors were used under conditions (cell line and time of exposure) in which

there was no evidence of intrinsic toxicity.
Based on these preliminary results, we decided to test the effect of ISRIB in both U937 and WT D-C2C12 cells exposed for 6, 16 or 24h to arsenite. The effect of EN460 was instead tested in similar experiments only in WT D-C2C12 cells. The results reported in the former Fig 4E (now Fig 4F) do not indicate that U937 cells are resistant to apoptosis induced by arsenite (which would be in obvious contrast with the data reported in Fig. 3). Rather, the effect of EN460 under these conditions was NOT TESTED (NT). To make it more clear, the new Fig 4F only presents 4 bars (control, arsenite and arsenite plus CsA or ISRIB).
Given the observed lack of toxicity of EN460 at 6 h, we tested the effect of EN460 on the DNA damaging response elicited by arsenite
We were impressed by high vulnerability of U937 cells to EN460, apparently shared by other hematological tumor cells (this point is commented in text of the revised version of the paper). We therefore agree with this reviewer that a very large proportion of these cells were metabolically dead at 16-24 h. For obvious reasons, we did not test the effects of EN460 in the arsenite-dependent toxicity parameters measured at 16 or 24 h.

2. The results section is divided in various sub-sections, as requested.
3. We performed the experiments requested and now present the results from Western blot studies in which cytochrome c immunoreactivity is measured in both the mitochondrial and cytosolic fractions.
4. This reviewer suggests to perform experiments to demonstrate that arsenite induces DNA strand scission via a ROS-dependent mechanism. However this information was given in a previous study from our laboratory (Guidarelli et al., Biofactors 2017), in which we also demonstrated the involvement of mitochondrial superoxide. This information is now reported in two different parts of the revised version of the manuscript.
5. We used one or two * to indicate that the response mediated by arsenite (alone or with other additions) is significantly different from that of untreated cells. In addition, one or two # indicate that the response of arsenite associated with various treatments is statistically different from that mediated by arsenite alone.

The title of Fig 5 was re-written.

Inhibition of activity/expression, or genetic deletion, of ERO1 α blunts arsenite geno- and cyto-toxicity

Andrea Guidarelli^a, Andrea Spina^a, Mara Fiorani^a, Ester Zito^{a,b} and Orazio Cantoni^{a*}

^a*Department of Biomolecular Sciences, University of Urbino Carlo Bo, Urbino, Italy.*

^b*Istituto di Ricerche Farmacologiche Mario Negri IRCCS, Milan, Italy*

***Corresponding author:** Prof. Orazio Cantoni, Dipartimento di Scienze Biomolecolari, Sezione di Farmacologia e Farmacognosia, Università degli Studi di Urbino, Via S. Chiara 27, 61029 Urbino (PU), Italy. Tel: +39-0722-303523; Fax: +39-0722-305470; e-mail: orazio.cantoni@uniurb.it

Abbreviations: 2-APB, 2-aminoethoxydiphenyl borate; Cf, caffeine; $[Ca^{2+}]_c$, cytosolic Ca^{2+} concentrations; $[Ca^{2+}]_m$, mitochondrial Ca^{2+} concentration; ER, endoplasmic reticulum; CsA, Cyclosporin A; ERO1 α , ER oxidoreductin1 α ; ERO1 α KO D-C2C12, ERO1 α KO differentiated C2C12 myotubes; IP₃R, inositol 1,4,5-trisphosphate receptor; mitoO₂⁻, mitochondrial superoxide; MCU, mitochondrial Ca^{2+} uniporter; MPT, mitochondrial permeability transition; Ry, ryanodine; RyR, ryanodine receptor; ROS, reactive oxygen species; WT D-C2C12, Wild Type differentiated C2C12 myotubes.

ABSTRACT

Our recent studies suggest that arsenite stimulates the crosstalk between the inositol 1, 4, 5-triphosphate receptor (IP₃R) and the ryanodine receptor (RyR) *via* a mechanism dependent on endoplasmic reticulum (ER) oxidoreductin1 α (ERO1 α) up-regulation. Under these conditions, **the fraction of Ca²⁺ released by the RyR *via* an ERO1 α -dependent mechanism** was promptly cleared by the mitochondria and critically mediated O₂⁻ formation, responsible for the triggering of time-dependent events associated with strand scission of genomic DNA and delayed mitochondrial apoptosis. We herein report that, in differentiated C2C12 cells, this sequence of events can be intercepted by genetic deletion of ERO1 α as well as by EN460, an inhibitor of ERO1 α activity. Similar results were obtained for the early effects mediated by arsenite in proliferating U937 cells, in which however the long-term studies were hampered by the intrinsic toxicity of the inhibitor. **It was then interesting to observe that ISRIB, an inhibitor of p-eIF2 alpha, was in both cell types devoid of intrinsic toxicity and able to suppress ERO1 α expression and the resulting downstream effects leading to arsenite geno- and cyto-toxicity. We therefore conclude that pharmacological inhibition of ERO1 α activity, or expression, effectively counteracts the deleterious effects induced by the metalloid *via* a mechanism associated with prevention of mitochondrial O₂⁻ formation.**

Keywords: arsenite; ERO1 α ; mitochondrial Ca²⁺; mitochondrial superoxide; DNA damage; apoptosis.

1. Introduction

Arsenite is a ubiquitous environmental contaminant with potent carcinogenic and toxic properties (Flora, 2011; Jomova et al., 2011; Minatel et al., 2018; Nurchi et al., 2020). The molecular mechanisms involved in these responses, still poorly understood, are conditioned by the ability of the metalloid to bind to protein thiols (Nurchi et al., 2020; Shen et al., 2013; Vergara-Geronimo et al., 2021) and to promote the formation of reactive oxygen species (ROS) (Flora, 2011; Hu et al., 2020; Jomova et al., 2011; Nurchi et al., 2020), **which may then contribute to the induction of numerous deleterious effects**. The overall scenario therefore appears rather confused, with many unanswered questions, further complicated by the existence of cell type and concentration-dependent mechanisms (Flora, 2011; Guidarelli et al., 2021; Hu et al., 2020).

With these considerations in mind, we initially developed a well-defined toxicity paradigm associated with mitochondrial superoxide (mitoO₂⁻) formation (Guidarelli et al., 2020; Guidarelli et al., 2019a). We found that these species are actively generated after exposure of U937 cells to low micromolar concentrations of arsenite *via* a mechanism critically regulated by Ca²⁺ (Guidarelli et al., 2021; Guidarelli et al., 2019a), thereby emphasizing the importance of parallel effects mediated by the metalloid in the endoplasmic reticulum (ER). More specifically, arsenite induced an initial stimulation of the inositol-1,4, 5-trisphosphate receptor (IP₃R), critically connected with the activation of the ryanodine receptor (RyR), finally responsible for the release of the fraction of Ca²⁺ accumulated by the mitochondria (Guidarelli et al., 2021; Guidarelli et al., 2019a). Interestingly, this sequence of events was observed in other cell types characterized by a similar functional organization of the ER/mitochondria network, including terminally differentiated C2C12 cells (Guidarelli et al., 2019a).

Recently, we reported that the above crosstalk between the IP₃R and RyR is regulated by ER oxidoreductin1α (ERO1α) (Spina et al., 2022). More specifically, arsenite promoted ERO1α **expression and its pharmacological or genetic inhibition** was associated with prevention of Ca²⁺

release from the RyR, the ensuing mitochondrial Ca^{2+} accumulation and the final mitoO_2^- formation (Spina et al., 2022).

Having previously demonstrated that arsenite-induced mitoO_2^- leads to an early DNA strand scission (Guidarelli et al., 2017), followed by mitochondrial dysfunction and mitochondrial permeability transition (MPT)-dependent apoptosis (Guidarelli et al., 2017), we challenged the hypothesis of preventing the deleterious effects of arsenite by targeting ERO1 α .

For this purpose we used EN460, an inhibitor of the reshuffling of electrons in ERO1 α , thereby blunting its redox activity (Blais et al., 2010; Hayes et al., 2019). In a recent study (Spina et al., 2022), **this inhibitor was successfully employed to infer a role** of ERO1 α in RyR activation after the stimulation of the IP₃R mediated by arsenite. In these experiments, however, EN460 was used at 10 μM and left in the cultures for 6 h, i.e., **under carefully selected conditions in which the impact of ERO1 α inhibition was not associated with** confounding toxic effects of the inhibitor. **On the other hand**, EN460 displays numerous off target effects (Blais et al., 2010; Hayes et al., 2019), thereby implying the possibility that longer times of incubation will eventually promote toxicity.

We therefore considered the possibility of limiting the impact of ERO1 α through the inhibition of its expression. ISRIB is a small molecule inhibiting the activity of p-eIF2 alpha and the expression of CHOP, which is upstream to ERO1 α in the PERK branch of the ER stress response (Sidrauski et al., 2015; Zyryanova et al., 2021). Most importantly, ISRIB is not particularly toxic in cultured cells (Hosoi et al., 2016; Koncha et al., 2021) and other preclinical models (Halliday et al., 2015; Wong et al., 2019), thereby suggesting the possibility of its use in humans (Rabouw et al., 2019; Schoof et al., 2021; Sidrauski et al., 2015).

Based on these considerations, we characterized the effects of ISRIB on arsenite-induced expression of ERO1 α , deregulation of Ca^{2+} **homeostasis and mitoO_2^- formation** in U937 and in Wild Type differentiated C2C12 cells (WT D-C2C12). We then performed an accurate characterization of the

toxic effects mediated by EN460, or ISRIB, over a 6-24 h exposure time-window, to finally address the issue of whether pharmacological inhibition of either the activity or expression of ERO1 α prevents the early DNA strand scission and the delayed MPT-dependent apoptosis induced by arsenite. The outcome of these inhibitor studies was compared with that of experiments using ERO1 α KO C2C12 myotubes (ERO1 α KO D-C2C12).

2. Materials and methods

2.1. Chemicals

Sodium arsenite, thapsigargin, 2-aminoethoxydiphenyl borate (2-APB), ryanodine (Ry), Hoechst 33342 as well as most of reagent-grade chemicals were purchased from Sigma-Aldrich (Milan, Italy). ISRIB and EN460 were obtained from Calbiochem (San Diego, CA). Cyclosporin A (CsA) was from Novartis (Bern, Switzerland). Fluo-4-acetoxymethyl ester, Rhod 2-acetoxymethyl ester and MitoSOX red were purchased from Thermo Fisher Scientific (Milan, Italy).

2.2. Cell culture

Human U937 promonocytic cells were cultured in RPMI 1640 medium (Sigma-Aldrich, Milan, Italy), supplemented with 10% fetal bovine serum (Euroclone, Celbio Biotecnologie, Milan, Italy), penicillin (100 units/ml) and streptomycin (100 µg/ml) (Euroclone), at 37 °C in T-75 tissue culture flasks (Corning Inc., Corning, NY, USA) gassed with an atmosphere of 95% air-5% CO₂.

Wild type (WT) and ERO1 α KO C2C12 myoblasts, generated as detailed in (Varone et al., 2019), were cultured in high-glucose D-MEM (Sigma-Aldrich) supplemented with 10% heat inactivated FBS, 2 mM L-glutamine (Euroclone). Proliferating WT and ERO1 α KO myoblasts had a similar morphology that in both circumstances changed significantly after 4 days of growth in D-MEM supplemented with 1% heat-inactivated serum. WT and ERO1 α KO myotubes (WT D-C2C12 and ERO1 α KO D-C2C12) also had a similar morphology. Remarkably similar was also the gain of expression of specific markers of differentiation, as increased myogenin and myosin (Spina et al., 2022). In addition, Western blot of the lysates provided evidence of ERO1 α expression in WT D-C2C12 cells but not in ERO1 α KO D-C2C12 cells (Spina et al., 2022).

2.3. Sub-cellular fractionation and western blot analysis

Cells were lysed with the addition of a buffer containing 50 mM Tris, 5mM EDTA, 150 mM NaCl, 0,5% Triton, 0,1% SDS, 1 mM DTT, 1 mM Na₃VO₄, 1 mM NaF, 350 mM PMSF, 1% protease

inhibitor complex, pH 7.5. In some experiments, the cells were processed to obtain the cytosolic and mitochondrial fractions, as previously described (Yu et al., 2003). 30 µg of proteins were loaded in each lane, separated by polyacrylamide gel electrophoresis in the presence of sodium dodecyl sulfate and transferred to polyvinylidene difluoride membranes. The membranes were blocked and incubated with antibodies against ERO1α (NB 100-2525, Atlas Antibodies, Stockholm Sweden), cytochrome c (sc-13560, Santa Cruz Biotechnology, Santa Cruz, CA) β-actin (VMA00048, Bio-Rad, Hercules, CA), and HSP-60 (sc-13115, Santa Cruz Biotechnology). Immunoblots were processed with horse-radish peroxidase-conjugated anti-rabbit (ERO1α) or anti-mouse (β-actin, cytochrome c and HSP-60) antibodies. Antibodies against β-actin and HSP-60 were used to assess the equal loading of the lanes and the purity of the fractions. Relative amounts of proteins were quantified by densitometric analysis using Image J software.

2.4. *Measurement of cytosolic and mitochondrial Ca²⁺ levels*

The cells were exposed to 4 µM Fluo-4-acetoxymethyl ester, or 10 µM Rhod 2-acetoxymethyl ester, in the last 30 min of the treatments. The cells were then washed with a phosphate buffer saline (PBS, 136 mM NaCl, 10 mM Na₂HPO₄, 1.5 mM KH₂PO₄, 3 mM KCl; pH 7.4) and processed for fluorescence microscopy analysis as previously detailed (Spina et al., 2022).

2.5. *MitoSOX red fluorescence assays*

The cells were exposed to 5 µM MitoSOX red in the last 30 min of the treatments. The cells were then washed with PBS and processed for fluorescence microscopy analysis as indicated in (Spina et al., 2022).

2.6. *Measurement of DNA single-strand breakage by the alkaline halo assay*

The formation of DNA single-strand breaks was determined using the alkaline halo assay. Details on the method, processing of fluorescence images and calculation of the experimental results are provided in (Cantoni and Guidarelli, 2008). The nuclear spreading factor value, represents the ratio

between the area of the halo (obtained by subtracting the area of the nucleus from the total area, nucleus + halo) and that of the nucleus, from 50 to 75 randomly selected cells/experiment/treatment condition. Results are expressed as relative nuclear spreading factor values calculated by subtracting the nuclear spreading factor values of control cells from those of treated cells.

2.7. Measurement of mitochondrial membrane potential

Cells were exposed to 50 nM MitoTracker Red CMXRos in the last 30 min of the treatments. The cells were then washed with PBS and processed for fluorescence microscopy analysis as indicated in (Spina et al., 2022).

2.8. Immunofluorescence analysis

Cells were incubated for 16 h in the absence or presence of arsenite, fixed for 1 min with 95% ethanol/5% acetic acid, washed with PBS, and blocked in PBS-containing bovine serum albumin (2% w/v) (30 min at room temperature). The cells were subsequently incubated with monoclonal anti-cytochrome c antibodies (1:100 in PBS containing 2% bovine serum albumin; Santa Cruz Biotechnology) stored for 18 h at 4° C, washed and incubated for 3 h in the dark with fluorescein isothiocyanate (Santa Cruz Biotechnology)-conjugated secondary antibody diluted 1:100 in PBS. The cells were finally examined with a fluorescence microscope as indicated in (Spina et al., 2022).

2.9. Fluorogenic caspase 3 assay

Cells were exposed for 24 h to arsenite and then analysed for caspase 3-like activity as detailed in (Guidarelli et al., 2005). Caspase 3-like activity was determined fluorometrically (excitation at 360 nm and emission at 460 nm) by quantifying the release of aminomethylcoumarin (AMC) from cleaved caspase 3 substrate (Ac-DEVD-AMC).

2.10. Cytotoxicity assay

Cells were exposed for 24 h to arsenite and analysed with the trypan blue exclusion assay. Briefly, an aliquot of the cell suspension was diluted 1:2 (v/v) with 0.4% trypan blue, and the viable cells (i.e., those excluding trypan blue) were counted with a hemocytometer.

Toxicity was also determined using the MTT assay. In these experiments, the cells were supplemented with 25 µg/ml MTT in the last 30 min of the treatment with arsenite (24 h). After treatments, the cells were washed with PBS and the resulting formazan extracted with 1 ml of dimethyl sulfoxide. Absorbance was finally read at 570 nm.

2.11. Analysis of apoptosis with the Hoechst 33342 assay

Cells were incubated for 5 min with 10 µM Hoechst 33342 at the end of the 24 h exposure to arsenite, and accurately washed three times with PBS. Fluorescence microscopy analysis was performed to determine the relative numbers of cells presenting evidence of chromatin condensation or fragmentation (apoptotic cells) and cells with homogeneously stained nuclei (viable cells).

2.12. Statistical analysis

GraphPad Prism was used for statistical analysis. All quantitative Data were presented as the mean ± standard deviation (SD). Statistically significant differences were obtained using one-way ANOVA. A P value of <0.05 was considered statistically significant.

3. Results

3.1 ISRIB inhibits ERO1 α expression induced by arsenite, thereby preventing the ensuing effects on Ca²⁺ homeostasis and mitoO₂⁻ formation

The results illustrated in Fig. 1 indicate that a 6 h exposure of U937 cells (A and C), or D-C2C12 cells (B and D), to either thapsigargin (5 μ M) or arsenite (2.5 μ M), promotes quantitatively similar increases in ERO 1 α expression. Interestingly, ISRIB (200 nM) suppressed ERO 1 α expression induced in these different cell types and conditions.

We previously reported that in the above cell types arsenite increases the cytosolic concentration of Ca²⁺ ([Ca²⁺]_c) via a mechanism partially sensitive to 20 μ M Ry, or 10 μ M EN460 (Spina et al., 2022), employed under conditions respectively associated with suppression of Ca²⁺ mobilization induced by the RyR agonist Cf (Spina et al., 2022), or with inhibition of ERO1 α activity (Spina et al., 2022). Fig. 2A shows that the inhibitory responses mediated by Ry, or EN460, were mimicked by ISRIB. Importantly, at the concentrations and time of exposure indicated above, EN460 or ISRIB were not toxic for U937 and WT D-C2C12 cells.

In both cell types, the effects of arsenite on the [Ca²⁺]_c were paralleled by an increased mitochondrial concentration of the cation ([Ca²⁺]_m) (Fig. 2 B) and by the concomitant formation of mitoO₂⁻ (Fig. 2C). Both responses were suppressed by Ry, EN460 or ISRIB. In addition, arsenite failed to increase the [Ca²⁺]_m (Fig. 2B) and to elicit mitoO₂⁻ formation (Fig. 2C) in ERO1 α KO D-C2C12 cells. In these cells, arsenite promoted a modest increase in the [Ca²⁺]_c, insensitive to Ry, EN460 or ISRIB, and quantitatively similar to the one observed in WT D-C2C12 cells supplemented with the metalloid and each of these inhibitors (Fig. 2A).

The above results therefore indicate that ISRIB suppresses ERO1 α expression induced by arsenite, an event associated with prevention of Ca²⁺ release from the RyR and the ensuing mitochondrial accumulation of the cation critically connected to mitoO₂⁻ formation.

3.2. Pharmacological inhibition of ERO1 α expression or activity, or its genetic deletion, abolishes the early deleterious effects of arsenite

Based on the results illustrated in the previous section, we investigated the effects of Ry, EN460 or ISRIB on arsenite genotoxicity. In U937 or WT D-C2C12 cells, arsenite caused an early (6 h) formation of DNA single strand breaks (Fig. 2D), in both circumstances sensitive to Ry, EN460 or ISRIB. Consistently, ERO 1 α KO D-C2C12 cells were resistant to the DNA strand scission induced by the metalloid. These results are therefore in line with those from experiments measuring mitoO₂^{·-} formation (Fig. 2C), in which the suppressive effects of Ry were recapitulated by EN460, ISRIB as well as by deletion of ERO1 α .

In order to further establish the specificity of these findings, we performed experiments in which U937, WT D-C2C12 and ERO 1 α KO D-C2C12 cells were treated for 10 min with arsenite and Cf. We reasoned that Cf, by directly releasing Ca²⁺ from the RyR, thereby increasing the [Ca²⁺]_m, should bypass the ERO 1 α -dependent regulation of these effects culminating in mitoO₂^{·-} formation. This strategy was successfully employed to promote mitoO₂^{·-} formation under the same conditions in which arsenite alone failed to promote effects on Ca²⁺ homeostasis (Guidarelli et al., 2020).

Cf/arsenite indeed increased the [Ca²⁺]_c (Fig. 2E), [Ca²⁺]_m (Fig. 2F) and mitoO₂^{·-} formation (Fig. 2G). Identical ROS responses were obtained in U937, WT D-C2C12 and ERO 1 α KO D-C2C12 cells. In addition, mitoO₂^{·-} formation was under these different conditions invariably sensitive to Ry and insensitive to EN460 or ISRIB. In these experiments the cells were incubated for 6 h with the inhibitors, with the addition of the cocktail arsenite/Cf in the last 10 min.

In other experiments, we found that the 10 min exposure to Cf/arsenite promotes similar levels of DNA strand scission in U937 and WT D-C2C12 cells (Fig. 2H), which was significantly greater than that induced by a 6 h exposure to arsenite in the absence of Cf (Fig. 2D), suppressed by Ry and insensitive to EN460, or ISRIB. The final critical observation derived from these experiments was

that ERO 1 α KO D-C2C12 cells responded to Cf/arsenite with or without the above addition as their WT counterpart.

The outcome of the above experiments therefore argues against the possibility of off target effects of EN460, or ISRIB, and is therefore in keeping with the notion that chemical inhibition of the activity or expression of ERO 1 α represents an effective strategy to promote upstream inhibition of arsenite-induced mitoO₂⁻ formation and of the ensuing early formation of DNA single strand breaks.

3.3. Assessment of the intrinsic toxicity of EN460 or ISRIB

Having previously established that the early effects mediated by a low concentration of arsenite are followed by delayed MPT-dependent apoptosis (Guidarelli et al., 2021), we wondered whether the early protective effects of EN460 and ISRIB are associated with prevention of late cytotoxicity. In order to address this issue, we first performed toxicity studies in U937 (Fig. 3A, C, E) and WT D-C2C12 (Fig. 3B, D, F) cells exposed for increasing time intervals to 10 μ M EN460 or 200 nM ISRIB.

There was no evidence of toxicity at 6 h in the two cell types exposed to each of the inhibitors, as indicated by visual inspection of the cultures (not shown), and by the lack of effects on the number of viable cells (Fig. 3A and B), loss of membrane integrity (Fig. 3C and D) or apoptotic DNA condensation/fragmentation (Fig. 3E and F). There were instead remarkable differences at 16 and 24 h, in that only WT D-C2C12 cells remained viable after exposure to the inhibitors. U937 cells resulted particularly sensitive to EN460, and indeed displayed a time-dependent reduction in cell counts (Fig. 3A), as well as a progressive increase in the percentage of trypan blue positive (Fig. 3C) and apoptotic (Fig. 3E) cells.

Based on these findings, we decided to investigate whether ISRIB prevents the delayed toxic effects mediated by arsenite in U937 cells and in WT C2C12 myotubes. The effect of EN460 were instead investigated only in WT D-C2C12 cells.

3.4. Pharmacological inhibition of ERO1 α expression or activity, or its genetic deletion, abolishes the delayed toxic effects of arsenite

Prolonged exposure (16 h) of U937 cells or WT C2C12 myotubes to arsenite causes a decline in both the mitochondrial membrane potential (Fig. 4A) and MTT-reducing activity (Fig. 4B), as well as the mitochondrial loss of cytochrome c, which became clearly detectable in the cytosolic compartment (Fig. 4C). The cells were also analysed with a fluorescence microscope to determine the relative numbers of cells bearing a punctate vs diffused fluorescence. The first condition is indicative of a mitochondrial localization of cytochrome c, whereas the second provides evidence for a mitochondrial loss of cytochrome c. Arsenite significantly increased the percentage of U937 or WT D-C2C12 cells with a diffused fluorescence and this response (Fig. 4D), as well as the loss of mitochondrial membrane potential (Fig. 4A) and MTT-reducing activity (Fig. 4B) were suppressed by EN460, ISRIB or CsA. At 24 h, we obtained evidence of caspase 3 activation (Fig. 4E) and apoptotic DNA fragmentation/condensation (Fig. 4F), once again sensitive to EN460, ISRIB or CsA. The outcome of inhibitor studies was entirely consistent with the results obtained in experiments using ERO1 α KO D-C2C12 cells. Indeed, under these conditions, arsenite failed to promote a decline in mitochondrial membrane potential (Fig. 4A), loss of MTT-reducing activity (Fig. 4B) or mitochondrial cytochrome c (Fig. 4 C and D) at 16 h. Arsenite also failed to induce activation of caspase 3 (Fig. 4E) and apoptotic DNA fragmentation at 24 h (Fig. 4F).

We finally analyzed the same parameters in U937 cells, in which arsenite induced effects qualitatively and quantitatively similar to those mediated in WT D-C2C12 cells, and with an identical sensitivity to CsA or ISRIB. As previously mentioned, EN460 was not included in these studies because of its intrinsic toxicity.

The results obtained in these experiments, while emphasizing the pivotal role of ERO1 α in the regulation of events associated with arsenite-induced mitoO₂⁻ formation, indicate that inhibition of

ERO1 α activity or expression, or its genetic deletion, prevents delayed effects resulting in mitochondrial dysfunction and MPT-dependent apoptosis.

4. Discussion

The results presented in this study show that arsenite-induced DNA strand scission as well as mitochondrial dysfunction and apoptosis associated with the formation of mitoO₂⁻ can be prevented by strategies other than those based on pharmacological inhibition of MPT (Guidarelli et al., 2015; Guidarelli et al., 2019b; Guidarelli et al., 2017) or on antioxidant supplementation (Guidarelli et al., 2015; Guidarelli et al., 2019a, b; Guidarelli et al., 2017).

It is well established that CsA inhibits the opening of the permeability transition pores caused by mitochondrial ROS in an array of toxicity paradigms (Bauer and Murphy, 2020; Bonora et al., 2020) and consequently prevents the downstream apoptotic signaling, as we also report in this study for U937 and WT-D-C2C12 cells exposed for 16-24 h to a low concentration of arsenite. However, CsA failed to prevent arsenite-induced DNA strand scission observed at 6 h, a time at which there was no evidence of mitochondrial dysfunction and MPT.

Antioxidant supplementation can instead prevent the deleterious effects of arsenite *via* ROS scavenging, an observation previously made using high concentrations of general antioxidants (Flora, 2011; Kadirvel et al., 2007; Wang et al., 2013). On the other hand, the potential clinical significance of these findings is uncertain since translation of the experimental **results** obtained with antioxidants in cultured cells and animals to humans has very rarely proved to be successful (Ghezzi et al., 2017; Sies and Jones, 2020). A more specific strategy to target mitochondrial ROS would then be represented by treatments leading to increased antioxidant concentrations in the mitochondrial matrix (Apostolova and Victor, 2015; Jiang et al., 2020). This more specific approach was previously exploited in our laboratory (Fiorani et al., 2015) and took advantage of the discovery that cultured cells express functional Na⁺ dependent vitamin c transporter 2 in both the plasma and mitochondrial membranes (Fiorani et al., 2015). Moreover, the mitochondrial transporter of the vitamin is highly expressed in U937 cells and presents the same high affinity of its plasma membrane counterpart (Fiorani et al., 2015). As a consequence, short-term exposure to low micromolar concentrations of

L-ascorbic acid causes a dramatic increase in the mitochondrial concentration of the vitamin, under the same conditions in which its cytosolic levels were only marginally increased (Fiorani et al., 2015). Using these conditions, arsenite failed to produce detectable mitoO_2^- as well as the ensuing geno- and cyto-toxic effects (Guidarelli et al., 2015; Guidarelli et al., 2019a, b; Guidarelli et al., 2017). Although the high affinity mitochondrial transport of L-ascorbic acid is a likely “cell culture effect” (Cantoni et al., 2018), since cells are normally grown in the virtual absence of the vitamin, it appears nevertheless reasonable to predict that mitochondria targeted antioxidants (Apostolova and Victor, 2015; Jiang et al., 2020) may represent effective strategies to counteract mitochondrial ROS elicited by arsenite.

The approach herein exploited **to blunt DNA strand scission** and mitochondrial apoptosis induced by arsenite lies on effects upstream to mitoO_2^- formation, in particular associated with events critically regulated by ERO1 α . Indeed, arsenite promotes the formation of mitoO_2^- *via* a Ca^{2+} -dependent mechanism and **the mitochondrial fraction of the cation is** derived from the RyR recruited after the initial stimulation of the IP₃R *via* an ERO1 α -dependent mechanism.

In our initial experiments, we demonstrated that arsenite and thapsigargin similarly upregulated ERO1 α in proliferating U937 cells and terminally differentiated C2C12 cells. In addition, these responses were in both circumstances sensitive to ISRIB. As a consequence, ISRIB recapitulated all the effects mediated by EN460, or Ry, on the $[\text{Ca}^{2+}]_c$, $[\text{Ca}^{2+}]_m$ and mitoO_2^- formation stimulated by arsenite. **Importantly, the outcome of these studies was entirely consistent with that of experiments using ERO1 α KO cells.**

The specificity of the effects of EN460 and ISRIB was also established in experiments in which the ERO1 α -dependence for RyR stimulation was bypassed with the use of a RyR agonist. Cf was therefore employed to directly mobilize Ca^{2+} from the RyR, thereby **increasing the $[\text{Ca}^{2+}]_m$ and promoting** mitoO_2^- formation after a 10 min exposure to arsenite, otherwise unable to generate

detectable effects under these conditions. As we recently reported, a very short time of exposure to low concentrations of arsenite is indeed sufficient to promote significant effects in the mitochondrial respiratory chain, resulting in mitoO_2^- formation under conditions of increased $[\text{Ca}^{2+}]_m$ (Guidarelli et al., 2020). These responses were sensitive to Ry, as expected, but insensitive to EN460 or ISRIB, thereby suggesting that the responses mediated by these inhibitors in the 6 h arsenite exposure paradigm were not due to off-target effects.

Thus, the above results indicate that ISRIB prevents arsenite-dependent ERO1 α expression and the downstream effects on Ca^{2+} homeostasis and mitoO_2^- formation.

In order to employ appropriate conditions to test the impact of ISRIB and EN460 on the deleterious effects mediated by arsenite, we performed preliminary toxicity studies providing two important findings. The first one was that prolonged exposure to ISRIB fails to cause detectable toxicity in proliferating U937 cells and terminally differentiated C2C12 cells, two cell types bearing remarkably different characteristics. Thus, as previously suggested in other investigations (Halliday et al., 2015; Hosoi et al., 2016; Koncha et al., 2021; Wong et al., 2019), this inhibitor can be employed also in long-term exposure studies. The second finding was that EN460 instead promotes time- and cell type-dependent toxic effects, since the same lack of toxicity was restricted to WT D-C2C12 cells. In U937 cells, EN460 failed to affect viability in the first 6 h of exposure, but subsequently caused a time-dependent induction of both necrotic and apoptotic death. We consider unlikely the possibility that the susceptibility of U937 cells to prolonged exposure to EN460 is causally linked to the proliferation phenotype. Rather, their vulnerability is more likely related to some specific characteristics of leukemic cells, as previously suggested (Hayes et al., 2019).

Based on the above information, we restricted the use of EN460 to experiments in which the inhibitor was devoid of intrinsic toxicity.

We found that EN460 and ISRIB abolish the DNA strand scission induced by arsenite at 6 h in both cell types. In addition, these inhibitors were as effective as the MPT inhibitor CsA in preventing the delayed onset of mitochondrial dysfunction and apoptotic DNA fragmentation/condensation induced by the metalloid in WT D-C2C12 cells. Finally, ISRIB also prevented these delayed effects of arsenite in U937 cells. The specificity of the cytoprotective effects of EN460 and ISRIB is emphasized by the observation that, under identical conditions, the metalloid failed to promote DNA strand scission, mitochondrial dysfunction and apoptosis in ERO1 α KO D-C2C12 cells.

In conclusion, it appears that EN460 and ISRIB mimic the protective effects mediated by the ERO1 α KO phenotype, or by Ry, on Ca²⁺ mobilization/mitochondrial accumulation and mitoO₂⁻ formation induced by arsenite, thereby leading to suppression of the early DNA strand scission and late MTP-dependent apoptosis. The intrinsic toxicity of EN460, apparently cell type dependent, however sets a limitation to its potential use, whereas ISRIB appears particularly safe for both cell types. Pharmacological inhibitors of ERO1 α activity or expression therefore represent suitable candidates for challenging novel pharmacological strategies aimed at the prevention of arsenite-dependent geno- and cyto-toxicity associated with mitoO₂⁻ formation. The proposed mechanism whereby arsenite induces mitoO₂⁻-dependent DNA damage and mitochondrial apoptosis, as well as the specific targets of EN460 and ISRIB, are illustrated in Fig. 5.

Conflicts of interest

The authors declare no competing financial interest.

CRedit authorship contribution statement

Andrea Guidarelli: Investigation, coordinated the experiments, contributed to the design of the study, data curation, reviewed the manuscript. **Andrea Spina:** Investigation, data curation. **Ester Zito:** Investigation, data curation, reviewed the manuscript. **Mara Fiorani:** Investigation, data curation, reviewed the manuscript. **Orazio Cantoni:** Project administration, contributed to the design of the study, wrote, reviewed and edited the manuscript.

Declaration of competing interest

The authors declare that they have no known competing financial interests or personal relationships that could have appeared to influence the work reported in this paper.

Acknowledgements

This work was supported by Ministero dell'Università e della Ricerca Scientifica e Tecnologica, Programmi di Ricerca Scientifica di Rilevante Interesse Nazionale, 2017, [Grant number: 2017FJSM9S]. The authors thank Dr. Liana Cerioni for helpful advice and technical support.

References

- Apostolova, N., Victor, V.M., 2015. Molecular strategies for targeting antioxidants to mitochondria: therapeutic implications. *Antioxid. Redox Signal.* 22, 686-729.
- Bauer, T.M., Murphy, E., 2020. Role of Mitochondrial Calcium and the Permeability Transition Pore in Regulating Cell Death. *Circ. Res.* 126, 280-293.
- Blais, J.D., Chin, K.T., Zito, E., Zhang, Y., Heldman, N., Harding, H.P., Fass, D., Thorpe, C., Ron, D., 2010. A small molecule inhibitor of endoplasmic reticulum oxidation 1 (ERO1) with selectively reversible thiol reactivity. *J. Biol. Chem.* 285, 20993-21003.
- Bonora, M., Patergnani, S., Ramaccini, D., Morciano, G., Pedriali, G., Kahsay, A.E., Bouhamida, E., Giorgi, C., Wieckowski, M.R., Pinton, P., 2020. Physiopathology of the Permeability Transition Pore: Molecular Mechanisms in Human Pathology. *Biomolecules* 10, 998.
- Cantoni, O., Guidarelli, A., 2008. Indirect mechanisms of DNA strand scission by peroxynitrite. *Methods Enzymol.* 440, 111-120.
- Cantoni, O., Guidarelli, A., Fiorani, M., 2018. Mitochondrial Uptake and Accumulation of Vitamin C: What Can We Learn from Cell Culture Studies? *Antioxid. Redox Signal.* 29, 1502-1515.
- Fiorani, M., Azzolini, C., Cerioni, L., Scotti, M., Guidarelli, A., Ciacci, C., Cantoni, O., 2015. The mitochondrial transporter of ascorbic acid functions with high affinity in the presence of low millimolar concentrations of sodium and in the absence of calcium and magnesium. *Biochim. Biophys. Acta* 1848, 1393-1401.
- Flora, S.J., 2011. Arsenic-induced oxidative stress and its reversibility. *Free Radic. Biol. Med.* 51, 257-281.
- Ghezzi, P., Jaquet, V., Marcucci, F., Schmidt, H., 2017. The oxidative stress theory of disease: levels of evidence and epistemological aspects. *Br. J. Pharmacol.* 174, 1784-1796.
- Guidarelli, A., Catalani, A., Spina, A., Varone, E., Fumagalli, S., Zito, E., Fiorani, M., Cantoni, O., 2021. Functional organization of the endoplasmic reticulum dictates the susceptibility of target

cells to arsenite-induced mitochondrial superoxide formation, mitochondrial dysfunction and apoptosis. *Food Chem. Toxicol.* 156, 112523.

Guidarelli, A., Cerioni, L., Fiorani, M., Catalani, A., Cantoni, O., 2020. Arsenite-Induced Mitochondrial Superoxide Formation: Time and Concentration Requirements for the Effects of the Metalloid on the Endoplasmic Reticulum and Mitochondria. *J. Pharmacol. Exp. Ther.* 373, 62-71.

Guidarelli, A., Cerioni, L., Tommasini, I., Fiorani, M., Brune, B., Cantoni, O., 2005. Role of Bcl-2 in the arachidonate-mediated survival signaling preventing mitochondrial permeability transition-dependent U937 cell necrosis induced by peroxynitrite. *Free Radic. Biol. Med.* 39, 1638-1649.

Guidarelli, A., Fiorani, M., Azzolini, C., Cerioni, L., Scotti, M., Cantoni, O., 2015. U937 cell apoptosis induced by arsenite is prevented by low concentrations of mitochondrial ascorbic acid with hardly any effect mediated by the cytosolic fraction of the vitamin. *Biofactors* 41, 101-110.

Guidarelli, A., Fiorani, M., Carloni, S., Cerioni, L., Balduini, W., Cantoni, O., 2016. The study of the mechanism of arsenite toxicity in respiration-deficient cells reveals that NADPH oxidase-derived superoxide promotes the same downstream events mediated by mitochondrial superoxide in respiration-proficient cells. *Toxicol. Appl. Pharmacol.* 307, 35-44.

Guidarelli, A., Fiorani, M., Cerioni, L., Cantoni, O., 2019a. Calcium signals between the ryanodine receptor- and mitochondria critically regulate the effects of arsenite on mitochondrial superoxide formation and on the ensuing survival vs apoptotic signaling. *Redox Biol.* 20, 285-295.

Guidarelli, A., Fiorani, M., Cerioni, L., Cantoni, O., 2019b. The compartmentalised nature of the mechanisms governing superoxide formation and scavenging in cells exposed to arsenite. *Toxicol. Appl. Pharmacol.* 384, 114766.

- Guidarelli, A., Fiorani, M., Cerioni, L., Scotti, M., Cantoni, O., 2017. Arsenite induces DNA damage via mitochondrial ROS and induction of mitochondrial permeability transition. *Biofactors* 43, 673-684.
- Halliday, M., Radford, H., Sekine, Y., Moreno, J., Verity, N., le Quesne, J., Ortori, C.A., Barrett, D.A., Fromont, C., Fischer, P.M., Harding, H.P., Ron, D., Mallucci, G.R., 2015. Partial restoration of protein synthesis rates by the small molecule ISRIB prevents neurodegeneration without pancreatic toxicity. *Cell Death Dis.* 6, e1672.
- Hayes, K.E., Batsomboon, P., Chen, W.C., Johnson, B.D., Becker, A., Eschrich, S., Yang, Y., Robart, A.R., Dudley, G.B., Geldenhuys, W.J., Hazlehurst, L.A., 2019. Inhibition of the FAD containing ER oxidoreductin 1 (Ero1) protein by EN-460 as a strategy for treatment of multiple myeloma. *Bioorg. Med. Chem.* 27, 1479-1488.
- Hosoi, T., Kakimoto, M., Tanaka, K., Nomura, J., Ozawa, K., 2016. Unique pharmacological property of ISRIB in inhibition of Abeta-induced neuronal cell death. *J. Pharmacol. Sci.* 131, 292-295.
- Hu, Y., Li, J., Lou, B., Wu, R., Wang, G., Lu, C., Wang, H., Pi, J., Xu, Y., 2020. The Role of Reactive Oxygen Species in Arsenic Toxicity. *Biomolecules* 10, 240.
- Jiang, Q., Yin, J., Chen, J., Ma, X., Wu, M., Liu, G., Yao, K., Tan, B., Yin, Y., 2020. Mitochondria-Targeted Antioxidants: A Step towards Disease Treatment. *Oxid. Med. Cell. Longev.* 2020, 8837893.
- Jomova, K., Jenisova, Z., Feszterova, M., Baros, S., Liska, J., Hudecova, D., Rhodes, C.J., Valko, M., 2011. Arsenic: toxicity, oxidative stress and human disease. *J. Appl. Toxicol.* 31, 95-107.
- Kadirvel, R., Sundaram, K., Mani, S., Samuel, S., Elango, N., Panneerselvam, C., 2007. Supplementation of ascorbic acid and alpha-tocopherol prevents arsenic-induced protein oxidation and DNA damage induced by arsenic in rats. *Hum. Exp. Toxicol.* 26, 939-946.
- Koncha, R.R., Ramachandran, G., Sepuri, N.B.V., Ramaiah, K.V.A., 2021. CCCP-induced mitochondrial dysfunction - characterization and analysis of integrated stress response to cellular signaling and homeostasis. *FEBS J.* 288, 5737-5754.

- Minatel, B.C., Sage, A.P., Anderson, C., Hubaux, R., Marshall, E.A., Lam, W.L., Martinez, V.D., 2018. Environmental arsenic exposure: From genetic susceptibility to pathogenesis. *Environ. Int.* 112, 183-197.
- Nurchi, V.M., Djordjevic, A.B., Crisponi, G., Alexander, J., Bjorklund, G., Aaseth, J., 2020. Arsenic Toxicity: Molecular Targets and Therapeutic Agents. *Biomolecules* 10, 231.
- Rabouw, H.H., Langereis, M.A., Anand, A.A., Visser, L.J., de Groot, R.J., Walter, P., van Kuppeveld, F.J.M., 2019. Small molecule ISRIB suppresses the integrated stress response within a defined window of activation. *Proc. Natl. Acad. Sci. USA* 116, 2097-2102.
- Schoof, M., Boone, M., Wang, L., Lawrence, R., Frost, A., Walter, P., 2021. eIF2B conformation and assembly state regulate the integrated stress response. *ELife* 2021, 10, e65703.
- Shen, S., Li, X.F., Cullen, W.R., Weinfeld, M., Le, X.C., 2013. Arsenic binding to proteins. *Chem. Rev.* 113, 7769-7792.
- Sidrauski, C., McGeachy, A.M., Ingolia, N.T., Walter, P., 2015. The small molecule ISRIB reverses the effects of eIF2alpha phosphorylation on translation and stress granule assembly. *ELife* 2015, 4, e05033.
- Sies, H., Jones, D.P., 2020. Reactive oxygen species (ROS) as pleiotropic physiological signalling agents. *Nat. Rev. Mol. Cell Biol.* 21, 363-383.
- Spina, A., Guidarelli, A., Fiorani, M., Varone, E., Catalani, A., Zito, E., Cantoni, O., 2022. Crosstalk between ERO1alpha and ryanodine receptor in arsenite-dependent mitochondrial ROS formation. *Biochem. Pharmacol.* 198, 114973.
- Varone, E., Pozzer, D., Di Modica, S., Chernorudskiy, A., Nogara, L., Baraldo, M., Cinquanta, M., Fumagalli, S., Villar-Quiles, R.N., De Simoni, M.G., Blaauw, B., Ferreira, A., Zito, E., 2019. SELENON (SEPN1) protects skeletal muscle from saturated fatty acid-induced ER stress and insulin resistance. *Redox Biol.* 24, 101176.

- Vergara-Geronimo, C.A., Leon Del Rio, A., Rodriguez-Dorantes, M., Ostrosky-Wegman, P., Salazar, A.M., 2021. Arsenic-protein interactions as a mechanism of arsenic toxicity. *Toxicol. Appl. Pharmacol.* 431, 115738.
- Wang, F., Zhou, X., Liu, W., Sun, X., Chen, C., Hudson, L.G., Jian Liu, K., 2013. Arsenite-induced ROS/RNS generation causes zinc loss and inhibits the activity of poly(ADP-ribose) polymerase-1. *Free Radic. Biol. Med.* 61, 249-256.
- Wong, Y.L., LeBon, L., Basso, A.M., Kohlhaas, K.L., Nikkel, A.L., Robb, H.M., Donnelly-Roberts, D.L., Prakash, J., Swensen, A.M., Rubinstein, N.D., Krishnan, S., McAllister, F.E., Haste, N.V., O'Brien, J.J., Roy, M., Ireland, A., Frost, J.M., Shi, L., Riedmaier, S., Martin, K., Dart, M.J., Sidrauski, C., 2019. eIF2B activator prevents neurological defects caused by a chronic integrated stress response. *ELife* 2019, 8, e42940.
- Yu, W., Sanders, B. G. and Kline, K. (2003). RRR- α -tocopheryl succinate-induced apoptosis of human breast cancer cells involves Bax translocation to mitochondria. *Cancer Res.* 63, 2483-2491.
- Zyryanova, A.F., Kashiwagi, K., Rato, C., Harding, H.P., Crespillo-Casado, A., Perera, L.A., Sakamoto, A., Nishimoto, M., Yonemochi, M., Shirouzu, M., Ito, T., Ron, D., 2021. ISRIB Blunts the Integrated Stress Response by Allosterically Antagonising the Inhibitory Effect of Phosphorylated eIF2 on eIF2B. *Mol. Cell* 81, 88-103 e106.

Legend to the figures

Fig. 1. ISRIB inhibits ERO1 α expression induced by thapsigargin or arsenite

U937 (A,C) and WT D-C2C12 (B,D) cells were exposed for 6 h to 5 μ M thapsigargin (A,B) or 2.5 μ M arsenite (C,D), in the absence or presence of 200 nM ISRIB, and then analyzed for ERO1 α protein expression. Anti- β -actin antibody was used as a loading control. Results represent the means \pm SD calculated from at three separate experiments. *P <0.01, as compared to untreated cells. #P < 0.01, as compared to cells treated with thapsigargin or arsenite (ANOVA followed by Dunnett's test).

Fig. 2. ISRIB and EN460 recapitulate the effects of ryanodine on the [Ca²⁺]_c, [Ca²⁺]_m, mitochondrial superoxide formation and DNA damage induced by arsenite

U937, WT D-C2C12 and ERO1 α KO D-C2C12 cells were pretreated for 5 min with the vehicle, 20 μ M Ry, ISRIB or 10 μ M EN460 and incubated for 6 h with the further addition to arsenite. After treatments, the cells were analysed for Fluo 4 (A), Rhod 2 (B) and MitoSOX red (C) fluorescence as well as for DNA damage with the alkaline halo assay (D). In other experiments, cells exposed for 6 h to ISRIB, or EN460, were washed, re-suspended in fresh culture medium, loaded for 20 min with Fluo 4 (E), Rhod 2 (F), or MitoSOX red (G) and subsequently incubated for 10 min with 10 mM Cf and 2.5 μ M arsenite. After treatments, the cells were analyzed for their respective fluorescence responses (E-G) and for DNA damage (H). The results represent the means \pm SD calculated from at least three distinct experiments. *P <0.05, **P <0.01, as compared to untreated cells. #P < 0.05, ##P < 0.01, as compared to cells treated with arsenite (ANOVA followed by Dunnett's test).

Fig. 3. The effects of ISRIB or EN460 on U937 and WT D-C2C12 cell viability

U937 and WT D-C2C12 cells were exposed for increasing time intervals to ISRIB, or EN460, and then analysed by counting the number of viable cells (A) and trypan blue positive cells (B). Sister cultures were processed for the assessment of apoptotic chromatin fragmentation/condensation (C). The results represent the means \pm SD calculated from at least three distinct experiments. *P <0.05, **P <0.01, as compared to untreated cells. (ANOVA followed by Dunnett's test).

Fig. 4. *Arsenite causes mitochondrial dysfunction and apoptosis via mechanisms sensitive to inhibition of the activity or expression of ERO1 α , as well as to its genetic deletion*

U937, WT D-C2C12 and ERO1 α KO D-C2C12 cells were pretreated for 5 min with the vehicle, CsA, ISRIB or EN460, and incubated for 16 (A-D) or 24 (E,F) h with arsenite. After treatments, the cells were analysed for MitoTracker red CMXRos-fluorescence (A), MTT reducing activity (B), *cytochrome c (Cyt c) immunoreactivity in the cytosolic and mitochondrial fractions (C)*, cytochrome c localization (D), caspase 3 activity (E), or apoptotic chromatin fragmentation/condensation (F). The results represent the means \pm SD calculated from at least three distinct experiments. *P <0.05, **P <0.01, as compared to untreated cells. #P < 0.05, ##P < 0.01, as compared to cells treated with arsenite (ANOVA followed by Dunnett's test).

Fig. 5. *Proposed mechanism whereby EN460 and ISRIB inhibit DNA damage and mitochondrial apoptosis induced by a low concentration of arsenite.*

The metalloid promotes an initial activation of the IP₃R, which enhances the expression (sensitive to ISRIB) and activity (sensitive to EN460) of ERO1 α to critically regulate the activation of the RyR. Ca²⁺ release from the RyR (sensitive to Ry⁺) is associated with the mitochondrial accumulation of the cation and with the formation of mitoO₂⁻. Conversion of the latter to H₂O₂ leads to mitochondrial dysfunction and MPT-dependent apoptosis. The diffusible nature of H₂O₂ is also permissive for the

induction of distal effects, as DNA strand scission. Thus, ISRIB and EN460, by preventing the stimulatory effects of ERO1 α on the RyR prevent mitoO₂⁻ formation and its downstream effects leading to DNA strand scission and MPT-dependent apoptosis.

Inhibition of activity/expression, or genetic deletion, of ERO1 α blunts arsenite geno- and cyto-toxicity

Andrea Guidarelli^a, Andrea Spina^a, Mara Fiorani^a, Ester Zito^{a,b} and Orazio Cantoni^{a*}

^a*Department of Biomolecular Sciences, University of Urbino Carlo Bo, Urbino, Italy.*

^b*Istituto di Ricerche Farmacologiche Mario Negri IRCCS, Milan, Italy*

***Corresponding author:** Prof. Orazio Cantoni, Dipartimento di Scienze Biomolecolari, Sezione di Farmacologia e Farmacognosia, Università degli Studi di Urbino, Via S. Chiara 27, 61029 Urbino (PU), Italy. Tel: +39-0722-303523; Fax: +39-0722-305470; e-mail: orazio.cantoni@uniurb.it

Abbreviations: 2-APB, 2-aminoethoxydiphenyl borate; Cf, caffeine; $[Ca^{2+}]_c$, cytosolic Ca^{2+} concentrations; $[Ca^{2+}]_m$, mitochondrial Ca^{2+} concentration; ER, endoplasmic reticulum; CsA, Cyclosporin A; ERO1 α , ER oxidoreductin1 α ; ERO1 α KO D-C2C12, ERO1 α KO differentiated C2C12 myotubes; IP₃R, inositol 1,4,5-trisphosphate receptor; mitoO₂⁻, mitochondrial superoxide; MCU, mitochondrial Ca^{2+} uniporter; MPT, mitochondrial permeability transition; Ry, ryanodine; RyR, ryanodine receptor; ROS, reactive oxygen species; WT D-C2C12, Wild Type differentiated C2C12 myotubes.

ABSTRACT

Our recent studies suggest that arsenite stimulates the crosstalk between the inositol 1, 4, 5-triphosphate receptor (IP₃R) and the ryanodine receptor (RyR) *via* a mechanism dependent on endoplasmic reticulum (ER) oxidoreductin1 α (ERO1 α) up-regulation. Under these conditions, the fraction of Ca²⁺ released by the RyR *via* an ERO1 α -dependent mechanism was promptly cleared by the mitochondria and critically mediated O₂⁻ formation, responsible for the triggering of time-dependent events associated with strand scission of genomic DNA and delayed mitochondrial apoptosis. We herein report that, in differentiated C2C12 cells, this sequence of events can be intercepted by genetic deletion of ERO1 α as well as by EN460, an inhibitor of ERO1 α activity. Similar results were obtained for the early effects mediated by arsenite in proliferating U937 cells, in which however the long-term studies were hampered by the intrinsic toxicity of the inhibitor. It was then interesting to observe that ISRIB, an inhibitor of p-eIF2 alpha, was in both cell types devoid of intrinsic toxicity and able to suppress ERO1 α expression and the resulting downstream effects leading to arsenite geno- and cyto-toxicity. We therefore conclude that pharmacological inhibition of ERO1 α activity, or expression, effectively counteracts the deleterious effects induced by the metalloid *via* a mechanism associated with prevention of mitochondrial O₂⁻ formation.

Keywords: arsenite; ERO1 α ; mitochondrial Ca²⁺; mitochondrial superoxide; DNA damage; apoptosis.

1. Introduction

Arsenite is a ubiquitous environmental contaminant with potent carcinogenic and toxic properties (Flora, 2011; Jomova et al., 2011; Minatel et al., 2018; Nurchi et al., 2020). The molecular mechanisms involved in these responses, still poorly understood, are conditioned by the ability of the metalloid to bind to protein thiols (Nurchi et al., 2020; Shen et al., 2013; Vergara-Geronimo et al., 2021) and to promote the formation of reactive oxygen species (ROS) (Flora, 2011; Hu et al., 2020; Jomova et al., 2011; Nurchi et al., 2020), which may then contribute to the induction of numerous deleterious effects. The overall scenario therefore appears rather confused, with many unanswered questions, further complicated by the existence of cell type and concentration-dependent mechanisms (Flora, 2011; Guidarelli et al., 2021; Hu et al., 2020).

With these considerations in mind, we initially developed a well-defined toxicity paradigm associated with mitochondrial superoxide (mitoO_2^-) formation (Guidarelli et al., 2020; Guidarelli et al., 2019a). We found that these species are actively generated after exposure of U937 cells to low micromolar concentrations of arsenite *via* a mechanism critically regulated by Ca^{2+} (Guidarelli et al., 2021; Guidarelli et al., 2019a), thereby emphasizing the importance of parallel effects mediated by the metalloid in the endoplasmic reticulum (ER). More specifically, arsenite induced an initial stimulation of the inositol-1,4, 5-trisphosphate receptor (IP_3R), critically connected with the activation of the ryanodine receptor (RyR), finally responsible for the release of the fraction of Ca^{2+} accumulated by the mitochondria (Guidarelli et al., 2021; Guidarelli et al., 2019a). Interestingly, this sequence of events was observed in other cell types characterized by a similar functional organization of the ER/mitochondria network, including terminally differentiated C2C12 cells (Guidarelli et al., 2019a).

Recently, we reported that the above crosstalk between the IP_3R and RyR is regulated by ER oxidoreductin1 α (ERO1 α) (Spina et al., 2022). More specifically, arsenite promoted ERO1 α expression and its pharmacological or genetic inhibition was associated with prevention of Ca^{2+}

release from the RyR, the ensuing mitochondrial Ca^{2+} accumulation and the final mitoO_2^- formation (Spina et al., 2022).

Having previously demonstrated that arsenite-induced mitoO_2^- leads to an early DNA strand scission (Guidarelli et al., 2017), followed by mitochondrial dysfunction and mitochondrial permeability transition (MPT)-dependent apoptosis (Guidarelli et al., 2017), we challenged the hypothesis of preventing the deleterious effects of arsenite by targeting $\text{ERO1}\alpha$.

For this purpose we used EN460, an inhibitor of the reshuffling of electrons in $\text{ERO1}\alpha$, thereby blunting its redox activity (Blais et al., 2010; Hayes et al., 2019). In a recent study (Spina et al., 2022), this inhibitor was successfully employed to infer a role of $\text{ERO1}\alpha$ in RyR activation after the stimulation of the IP_3R mediated by arsenite. In these experiments, however, EN460 was used at 10 μM and left in the cultures for 6 h, i.e., under carefully selected conditions in which the impact of $\text{ERO1}\alpha$ inhibition was not associated with confounding toxic effects of the inhibitor. On the other hand, EN460 displays numerous off target effects (Blais et al., 2010; Hayes et al., 2019), thereby implying the possibility that longer times of incubation will eventually promote toxicity.

We therefore considered the possibility of limiting the impact of $\text{ERO1}\alpha$ through the inhibition of its expression. ISRIB is a small molecule inhibiting the activity of p-eIF2 alpha and the expression of CHOP, which is upstream to $\text{ERO1}\alpha$ in the PERK branch of the ER stress response (Sidrauski et al., 2015; Zyryanova et al., 2021). Most importantly, ISRIB is not particularly toxic in cultured cells (Hosoi et al., 2016; Koncha et al., 2021) and other preclinical models (Halliday et al., 2015; Wong et al., 2019), thereby suggesting the possibility of its use in humans (Rabouw et al., 2019; Schoof et al., 2021; Sidrauski et al., 2015).

Based on these considerations, we characterized the effects of ISRIB on arsenite-induced expression of $\text{ERO1}\alpha$, deregulation of Ca^{2+} homeostasis and mitoO_2^- formation in U937 and in Wild Type differentiated C2C12 cells (WT D-C2C12). We then performed an accurate characterization of the

toxic effects mediated by EN460, or ISRIB, over a 6-24 h exposure time-window, to finally address the issue of whether pharmacological inhibition of either the activity or expression of ERO1 α prevents the early DNA strand scission and the delayed MPT-dependent apoptosis induced by arsenite. The outcome of these inhibitor studies was compared with that of experiments using ERO1 α KO C2C12 myotubes (ERO1 α KO D-C2C12).

2. Materials and methods

2.1. Chemicals

Sodium arsenite, thapsigargin, 2-aminoethoxydiphenyl borate (2-APB), ryanodine (Ry), Hoechst 33342 as well as most of reagent-grade chemicals were purchased from Sigma-Aldrich (Milan, Italy). ISRIB and EN460 were obtained from Calbiochem (San Diego, CA). Cyclosporin A (CsA) was from Novartis (Bern, Switzerland). Fluo-4-acetoxymethyl ester, Rhod 2-acetoxymethyl ester and MitoSOX red were purchased from Thermo Fisher Scientific (Milan, Italy).

2.2. Cell culture

Human U937 promonocytic cells were cultured in RPMI 1640 medium (Sigma-Aldrich, Milan, Italy), supplemented with 10% fetal bovine serum (Euroclone, Celbio Biotecnologie, Milan, Italy), penicillin (100 units/ml) and streptomycin (100 µg/ml) (Euroclone), at 37 °C in T-75 tissue culture flasks (Corning Inc., Corning, NY, USA) gassed with an atmosphere of 95% air-5% CO₂.

Wild type (WT) and ERO1 α KO C2C12 myoblasts, generated as detailed in (Varone et al., 2019), were cultured in high-glucose D-MEM (Sigma-Aldrich) supplemented with 10% heat inactivated FBS, 2 mM L-glutamine (Euroclone). Proliferating WT and ERO1 α KO myoblasts had a similar morphology that in both circumstances changed significantly after 4 days of growth in D-MEM supplemented with 1% heat-inactivated serum. WT and ERO1 α KO myotubes (WT D-C2C12 and ERO1 α KO D-C2C12) also had a similar morphology. Remarkably similar was also the gain of expression of specific markers of differentiation, as increased myogenin and myosin (Spina et al., 2022). In addition, Western blot of the lysates provided evidence of ERO1 α expression in WT D-C2C12 cells but not in ERO1 α KO D-C2C12 cells (Spina et al., 2022).

2.3. Sub-cellular fractionation and western blot analysis

Cells were lysed with the addition of a buffer containing 50 mM Tris, 5mM EDTA, 150 mM NaCl, 0,5% Triton, 0,1% SDS, 1 mM DTT, 1 mM Na₃VO₄, 1 mM NaF, 350 mM PMSF, 1% protease

inhibitor complex, pH 7.5. In some experiments, the cells were processed to obtain the cytosolic and mitochondrial fractions, as previously described (Yu et al., 2003). 30 µg of proteins were loaded in each lane, separated by polyacrylamide gel electrophoresis in the presence of sodium dodecyl sulfate and transferred to polyvinylidene difluoride membranes. The membranes were blocked and incubated with antibodies against ERO1α (NB 100-2525, Atlas Antibodies, Stockholm Sweden), cytochrome c (sc-13560, Santa Cruz Biotechnology, Santa Cruz, CA) β-actin (VMA00048, Bio-Rad, Hercules, CA), and HSP-60 (sc-13115, Santa Cruz Biotechnology). Immunoblots were processed with horse-radish peroxidase-conjugated anti-rabbit (ERO1α) or anti-mouse (β-actin, cytochrome c and HSP-60) antibodies. Antibodies against β-actin and HSP-60 were used to assess the equal loading of the lanes and the purity of the fractions. Relative amounts of proteins were quantified by densitometric analysis using Image J software.

2.4. Measurement of cytosolic and mitochondrial Ca²⁺ levels

The cells were exposed to 4 µM Fluo-4-acetoxymethyl ester, or 10 µM Rhod 2-acetoxymethyl ester, in the last 30 min of the treatments. The cells were then washed with a phosphate buffer saline (PBS, 136 mM NaCl, 10 mM Na₂HPO₄, 1.5 mM KH₂PO₄, 3 mM KCl; pH 7.4) and processed for fluorescence microscopy analysis as previously detailed (Spina et al., 2022).

2.5. MitoSOX red fluorescence assays

The cells were exposed to 5 µM MitoSOX red in the last 30 min of the treatments. The cells were then washed with PBS and processed for fluorescence microscopy analysis as indicated in (Spina et al., 2022).

2.6. Measurement of DNA single-strand breakage by the alkaline halo assay

The formation of DNA single-strand breaks was determined using the alkaline halo assay. Details on the method, processing of fluorescence images and calculation of the experimental results are provided in (Cantoni and Guidarelli, 2008). The nuclear spreading factor value, represents the ratio

between the area of the halo (obtained by subtracting the area of the nucleus from the total area, nucleus + halo) and that of the nucleus, from 50 to 75 randomly selected cells/experiment/treatment condition. Results are expressed as relative nuclear spreading factor values calculated by subtracting the nuclear spreading factor values of control cells from those of treated cells.

2.7. Measurement of mitochondrial membrane potential

Cells were exposed to 50 nM MitoTracker Red CMXRos in the last 30 min of the treatments. The cells were then washed with PBS and processed for fluorescence microscopy analysis as indicated in (Spina et al., 2022).

2.8. Immunofluorescence analysis

Cells were incubated for 16 h in the absence or presence of arsenite, fixed for 1 min with 95% ethanol/5% acetic acid, washed with PBS, and blocked in PBS-containing bovine serum albumin (2% w/v) (30 min at room temperature). The cells were subsequently incubated with monoclonal anti-cytochrome c antibodies (1:100 in PBS containing 2% bovine serum albumin; Santa Cruz Biotechnology) stored for 18 h at 4° C, washed and incubated for 3 h in the dark with fluorescein isothiocyanate (Santa Cruz Biotechnology)-conjugated secondary antibody diluted 1:100 in PBS. The cells were finally examined with a fluorescence microscope as indicated in (Spina et al., 2022).

2.9. Fluorogenic caspase 3 assay

Cells were exposed for 24 h to arsenite and then analysed for caspase 3-like activity as detailed in (Guidarelli et al., 2005). Caspase 3-like activity was determined fluorometrically (excitation at 360 nm and emission at 460 nm) by quantifying the release of aminomethylcoumarin (AMC) from cleaved caspase 3 substrate (Ac-DEVD-AMC).

2.10. Cytotoxicity assay

Cells were exposed for 24 h to arsenite and analysed with the trypan blue exclusion assay. Briefly, an aliquot of the cell suspension was diluted 1:2 (v/v) with 0.4% trypan blue, and the viable cells (i.e., those excluding trypan blue) were counted with a hemocytometer.

Toxicity was also determined using the MTT assay. In these experiments, the cells were supplemented with 25 µg/ml MTT in the last 30 min of the treatment with arsenite (24 h). After treatments, the cells were washed with PBS and the resulting formazan extracted with 1 ml of dimethyl sulfoxide. Absorbance was finally read at 570 nm.

2.11. Analysis of apoptosis with the Hoechst 33342 assay

Cells were incubated for 5 min with 10 µM Hoechst 33342 at the end of the 24 h exposure to arsenite, and accurately washed three times with PBS. Fluorescence microscopy analysis was performed to determine the relative numbers of cells presenting evidence of chromatin condensation or fragmentation (apoptotic cells) and cells with homogeneously stained nuclei (viable cells).

2.12. Statistical analysis

GraphPad Prism was used for statistical analysis. All quantitative Data were presented as the mean ± standard deviation (SD). Statistically significant differences were obtained using one-way ANOVA. A P value of <0.05 was considered statistically significant.

3. Results

3.1 ISRIB inhibits ERO1 α expression induced by arsenite, thereby preventing the ensuing effects on Ca²⁺ homeostasis and mitoO₂⁻ formation

The results illustrated in Fig. 1 indicate that a 6 h exposure of U937 cells (A and C), or D-C2C12 cells (B and D), to either thapsigargin (5 μ M) or arsenite (2.5 μ M), promotes quantitatively similar increases in ERO 1 α expression. Interestingly, ISRIB (200 nM) suppressed ERO 1 α expression induced in these different cell types and conditions.

We previously reported that in the above cell types arsenite increases the cytosolic concentration of Ca²⁺ ([Ca²⁺]_c) *via* a mechanism partially sensitive to 20 μ M Ry, or 10 μ M EN460 (Spina et al., 2022), employed under conditions respectively associated with suppression of Ca²⁺ mobilization induced by the RyR agonist Cf (Spina et al., 2022), or with inhibition of ERO1 α activity (Spina et al., 2022). Fig. 2A shows that the inhibitory responses mediated by Ry, or EN460, were mimicked by ISRIB. Importantly, at the concentrations and time of exposure indicated above, EN460 or ISRIB were not toxic for U937 and WT D-C2C12 cells.

In both cell types, the effects of arsenite on the [Ca²⁺]_c were paralleled by an increased mitochondrial concentration of the cation ([Ca²⁺]_m) (Fig. 2 B) and by the concomitant formation of mitoO₂⁻ (Fig. 2C). Both responses were suppressed by Ry, EN460 or ISRIB. In addition, arsenite failed to increase the [Ca²⁺]_m (Fig. 2B) and to elicit mitoO₂⁻ formation (Fig. 2C) in ERO1 α KO D-C2C12 cells. In these cells, arsenite promoted a modest increase in the [Ca²⁺]_c, insensitive to Ry, EN460 or ISRIB, and quantitatively similar to the one observed in WT D-C2C12 cells supplemented with the metalloid and each of these inhibitors (Fig. 2A).

The above results therefore indicate that ISRIB suppresses ERO1 α expression induced by arsenite, an event associated with prevention of Ca²⁺ release from the RyR and the ensuing mitochondrial accumulation of the cation critically connected to mitoO₂⁻ formation.

3.2. Pharmacological inhibition of ERO1 α expression or activity, or its genetic deletion, abolishes the early deleterious effects of arsenite

Based on the results illustrated in the previous section, we investigated the effects of Ry, EN460 or ISRIB on arsenite genotoxicity. In U937 or WT D-C2C12 cells, arsenite caused an early (6 h) formation of DNA single strand breaks (Fig. 2D), in both circumstances sensitive to Ry, EN460 or ISRIB. Consistently, ERO 1 α KO D-C2C12 cells were resistant to the DNA strand scission induced by the metalloid. These results are therefore in line with those from experiments measuring mitoO₂^{·-} formation (Fig. 2C), in which the suppressive effects of Ry were recapitulated by EN460, ISRIB as well as by deletion of ERO 1 α .

In order to further establish the specificity of these findings, we performed experiments in which U937, WT D-C2C12 and ERO 1 α KO D-C2C12 cells were treated for 10 min with arsenite and Cf. We reasoned that Cf, by directly releasing Ca²⁺ from the RyR, thereby increasing the [Ca²⁺]_m, should bypass the ERO 1 α -dependent regulation of these effects culminating in mitoO₂^{·-} formation. This strategy was successfully employed to promote mitoO₂^{·-} formation under the same conditions in which arsenite alone failed to promote effects on Ca²⁺ homeostasis (Guidarelli et al., 2020).

Cf/arsenite indeed increased the [Ca²⁺]_c (Fig. 2E), [Ca²⁺]_m (Fig. 2F) and mitoO₂^{·-} formation (Fig. 2G). Identical ROS responses were obtained in U937, WT D-C2C12 and ERO 1 α KO D-C2C12 cells. In addition, mitoO₂^{·-} formation was under these different conditions invariably sensitive to Ry and insensitive to EN460 or ISRIB. In these experiments the cells were incubated for 6 h with the inhibitors, with the addition of the cocktail arsenite/Cf in the last 10 min.

In other experiments, we found that the 10 min exposure to Cf/arsenite promotes similar levels of DNA strand scission in U937 and WT D-C2C12 cells (Fig. 2H), which was significantly greater than that induced by a 6 h exposure to arsenite in the absence of Cf (Fig. 2D), suppressed by Ry and insensitive to EN460, or ISRIB. The final critical observation derived from these experiments was

that ERO 1 α KO D-C2C12 cells responded to Cf/arsenite with or without the above addition as their WT counterpart.

The outcome of the above experiments therefore argues against the possibility of off target effects of EN460, or ISRIB, and is therefore in keeping with the notion that chemical inhibition of the activity or expression of ERO1 α represents an effective strategy to promote upstream inhibition of arsenite-induced mitoO₂⁻ formation and of the ensuing early formation of DNA single strand breaks.

3.3. Assessment of the intrinsic toxicity of EN460 or ISRIB

Having previously established that the early effects mediated by a low concentration of arsenite are followed by delayed MPT-dependent apoptosis (Guidarelli et al., 2021), we wondered whether the early protective effects of EN460 and ISRIB are associated with prevention of late cytotoxicity. In order to address this issue, we first performed toxicity studies in U937 (Fig. 3A, C, E) and WT D-C2C12 (Fig. 3B, D, F) cells exposed for increasing time intervals to 10 μ M EN460 or 200 nM ISRIB.

There was no evidence of toxicity at 6 h in the two cell types exposed to each of the inhibitors, as indicated by visual inspection of the cultures (not shown), and by the lack of effects on the number of viable cells (Fig. 3A and B), loss of membrane integrity (Fig. 3C and D) or apoptotic DNA condensation/fragmentation (Fig. 3E and F). There were instead remarkable differences at 16 and 24 h, in that only WT D-C2C12 cells remained viable after exposure to the inhibitors. U937 cells resulted particularly sensitive to EN460, and indeed displayed a time-dependent reduction in cell counts (Fig. 3A), as well as a progressive increase in the percentage of trypan blue positive (Fig. 3C) and apoptotic (Fig. 3E) cells.

Based on these findings, we decided to investigate whether ISRIB prevents the delayed toxic effects mediated by arsenite in U937 cells and in WT C2C12 myotubes. The effect of EN460 were instead investigated only in WT D-C2C12 cells.

3.4. Pharmacological inhibition of ERO 1 α expression or activity, or its genetic deletion, abolishes the delayed toxic effects of arsenite

Prolonged exposure (16 h) of U937 cells or WT C2C12 myotubes to arsenite causes a decline in both the mitochondrial membrane potential (Fig. 4A) and MTT-reducing activity (Fig. 4B), as well as the mitochondrial loss of cytochrome c, which became clearly detectable in the cytosolic compartment (Fig. 4C). The cells were also analysed with a fluorescence microscope to determine the relative numbers of cells bearing a punctate vs diffused fluorescence. The first condition is indicative of a mitochondrial localization of cytochrome c, whereas the second provides evidence for a mitochondrial loss of cytochrome c. Arsenite significantly increased the percentage of U937 or WT D-C2C12 cells with a diffused fluorescence and this response (Fig. 4D), as well as the loss of mitochondrial membrane potential (Fig. 4A) and MTT-reducing activity (Fig. 4B) were suppressed by EN460, ISRIB or CsA. At 24 h, we obtained evidence of caspase 3 activation (Fig. 4E) and apoptotic DNA fragmentation/condensation (Fig. 4F), once again sensitive to EN460, ISRIB or CsA. The outcome of inhibitor studies was entirely consistent with the results obtained in experiments using ERO1 α KO D-C2C12 cells. Indeed, under these conditions, arsenite failed to promote a decline in mitochondrial membrane potential (Fig. 4A), loss of MTT-reducing activity (Fig. 4B) or mitochondrial cytochrome c (Fig. 4 C and D) at 16 h. Arsenite also failed to induce activation of caspase 3 (Fig. 4E) and apoptotic DNA fragmentation at 24 h (Fig. 4F).

We finally analyzed the same parameters in U937 cells, in which arsenite induced effects qualitatively and quantitatively similar to those mediated in WT D-C2C12 cells, and with an identical sensitivity to CsA or ISRIB. As previously mentioned, EN460 was not included in these studies because of its intrinsic toxicity.

The results obtained in these experiments, while emphasizing the pivotal role of ERO1 α in the regulation of events associated with arsenite-induced mitoO₂⁻ formation, indicate that inhibition of

ERO1 α activity or expression, or its genetic deletion, prevents delayed effects resulting in mitochondrial dysfunction and MPT-dependent apoptosis.

4. Discussion

The results presented in this study show that arsenite-induced DNA strand scission as well as mitochondrial dysfunction and apoptosis associated with the formation of mitoO₂⁻ can be prevented by strategies other than those based on pharmacological inhibition of MPT (Guidarelli et al., 2015; Guidarelli et al., 2019b; Guidarelli et al., 2017) or on antioxidant supplementation (Guidarelli et al., 2015; Guidarelli et al., 2019a, b; Guidarelli et al., 2017).

It is well established that CsA inhibits the opening of the permeability transition pores caused by mitochondrial ROS in an array of toxicity paradigms (Bauer and Murphy, 2020; Bonora et al., 2020) and consequently prevents the downstream apoptotic signaling, as we also report in this study for U937 and WT-D-C2C12 cells exposed for 16-24 h to a low concentration of arsenite. However, CsA failed to prevent arsenite-induced DNA strand scission observed at 6 h, a time at which there was no evidence of mitochondrial dysfunction and MPT.

Antioxidant supplementation can instead prevent the deleterious effects of arsenite *via* ROS scavenging, an observation previously made using high concentrations of general antioxidants (Flora, 2011; Kadirvel et al., 2007; Wang et al., 2013). On the other hand, the potential clinical significance of these findings is uncertain since translation of the experimental results obtained with antioxidants in cultured cells and animals to humans has very rarely proved to be successful (Ghezzi et al., 2017; Sies and Jones, 2020). A more specific strategy to target mitochondrial ROS would then be represented by treatments leading to increased antioxidant concentrations in the mitochondrial matrix (Apostolova and Victor, 2015; Jiang et al., 2020). This more specific approach was previously exploited in our laboratory (Fiorani et al., 2015) and took advantage of the discovery that cultured cells express functional Na⁺ dependent vitamin c transporter 2 in both the plasma and mitochondrial membranes (Fiorani et al., 2015). Moreover, the mitochondrial transporter of the vitamin is highly expressed in U937 cells and presents the same high affinity of its plasma membrane counterpart (Fiorani et al., 2015). As a consequence, short-term exposure to low micromolar concentrations of

L-ascorbic acid causes a dramatic increase in the mitochondrial concentration of the vitamin, under the same conditions in which its cytosolic levels were only marginally increased (Fiorani et al., 2015). Using these conditions, arsenite failed to produce detectable mitoO_2^- as well as the ensuing geno- and cyto-toxic effects (Guidarelli et al., 2015; Guidarelli et al., 2019a, b; Guidarelli et al., 2017). Although the high affinity mitochondrial transport of L-ascorbic acid is a likely “cell culture effect” (Cantoni et al., 2018), since cells are normally grown in the virtual absence of the vitamin, it appears nevertheless reasonable to predict that mitochondria targeted antioxidants (Apostolova and Victor, 2015; Jiang et al., 2020) may represent effective strategies to counteract mitochondrial ROS elicited by arsenite.

The approach herein exploited to blunt DNA strand scission and mitochondrial apoptosis induced by arsenite lies on effects upstream to mitoO_2^- formation, in particular associated with events critically regulated by ERO1 α . Indeed, arsenite promotes the formation of mitoO_2^- *via* a Ca^{2+} -dependent mechanism and the mitochondrial fraction of the cation is derived from the RyR recruited after the initial stimulation of the IP₃R *via* an ERO1 α -dependent mechanism.

In our initial experiments, we demonstrated that arsenite and thapsigargin similarly upregulated ERO1 α in proliferating U937 cells and terminally differentiated C2C12 cells. In addition, these responses were in both circumstances sensitive to ISRIB. As a consequence, ISRIB recapitulated all the effects mediated by EN460, or Ry, on the $[\text{Ca}^{2+}]_c$, $[\text{Ca}^{2+}]_m$ and mitoO_2^- formation stimulated by arsenite. Importantly, the outcome of these studies was entirely consistent with that of experiments using ERO1 α KO cells.

The specificity of the effects of EN460 and ISRIB was also established in experiments in which the ERO1 α -dependence for RyR stimulation was bypassed with the use of a RyR agonist. Cf was therefore employed to directly mobilize Ca^{2+} from the RyR, thereby increasing the $[\text{Ca}^{2+}]_m$ and promoting mitoO_2^- formation after a 10 min exposure to arsenite, otherwise unable to generate

detectable effects under these conditions. As we recently reported, a very short time of exposure to low concentrations of arsenite is indeed sufficient to promote significant effects in the mitochondrial respiratory chain, resulting in mitoO_2^- formation under conditions of increased $[\text{Ca}^{2+}]_m$ (Guidarelli et al., 2020). These responses were sensitive to Ry, as expected, but insensitive to EN460 or ISRIB, thereby suggesting that the responses mediated by these inhibitors in the 6 h arsenite exposure paradigm were not due to off-target effects.

Thus, the above results indicate that ISRIB prevents arsenite-dependent ERO1 α expression and the downstream effects on Ca^{2+} homeostasis and mitoO_2^- formation.

In order to employ appropriate conditions to test the impact of ISRIB and EN460 on the deleterious effects mediated by arsenite, we performed preliminary toxicity studies providing two important findings. The first one was that prolonged exposure to ISRIB fails to cause detectable toxicity in proliferating U937 cells and terminally differentiated C2C12 cells, two cell types bearing remarkably different characteristics. Thus, as previously suggested in other investigations (Halliday et al., 2015; Hosoi et al., 2016; Koncha et al., 2021; Wong et al., 2019), this inhibitor can be employed also in long-term exposure studies. The second finding was that EN460 instead promotes time- and cell type-dependent toxic effects, since the same lack of toxicity was restricted to WT D-C2C12 cells. In U937 cells, EN460 failed to affect viability in the first 6 h of exposure, but subsequently caused a time-dependent induction of both necrotic and apoptotic death. We consider unlikely the possibility that the susceptibility of U937 cells to prolonged exposure to EN460 is causally linked to the proliferation phenotype. Rather, their vulnerability is more likely related to some specific characteristics of leukemic cells, as previously suggested (Hayes et al., 2019).

Based on the above information, we restricted the use of EN460 to experiments in which the inhibitor was devoid of intrinsic toxicity.

We found that EN460 and ISRIB abolish the DNA strand scission induced by arsenite at 6 h in both cell types. In addition, these inhibitors were as effective as the MPT inhibitor CsA in preventing the delayed onset of mitochondrial dysfunction and apoptotic DNA fragmentation/condensation induced by the metalloid in WT D-C2C12 cells. Finally, ISRIB also prevented these delayed effects of arsenite in U937 cells. The specificity of the cytoprotective effects of EN460 and ISRIB is emphasized by the observation that, under identical conditions, the metalloid failed to promote DNA strand scission, mitochondrial dysfunction and apoptosis in ERO1 α KO D-C2C12 cells.

In conclusion, it appears that EN460 and ISRIB mimic the protective effects mediated by the ERO1 α KO phenotype, or by Ry, on Ca²⁺ mobilization/mitochondrial accumulation and mitoO₂⁻ formation induced by arsenite, thereby leading to suppression of the early DNA strand scission and late MTP-dependent apoptosis. The intrinsic toxicity of EN460, apparently cell type dependent, however sets a limitation to its potential use, whereas ISRIB appears particularly safe for both cell types. Pharmacological inhibitors of ERO1 α activity or expression therefore represent suitable candidates for challenging novel pharmacological strategies aimed at the prevention of arsenite-dependent geno- and cyto-toxicity associated with mitoO₂⁻ formation. The proposed mechanism whereby arsenite induces mitoO₂⁻-dependent DNA damage and mitochondrial apoptosis, as well as the specific targets of EN460 and ISRIB, are illustrated in Fig. 5.

Conflicts of interest

The authors declare no competing financial interest.

CRedit authorship contribution statement

Andrea Guidarelli: Investigation, coordinated the experiments, contributed to the design of the study, data curation, reviewed the manuscript. **Andrea Spina:** Investigation, data curation. **Ester Zito:** Investigation, data curation, reviewed the manuscript. **Mara Fiorani:** Investigation, data curation, reviewed the manuscript. **Orazio Cantoni:** Project administration, contributed to the design of the study, wrote, reviewed and edited the manuscript.

Declaration of competing interest

The authors declare that they have no known competing financial interests or personal relationships that could have appeared to influence the work reported in this paper.

Acknowledgements

This work was supported by Ministero dell'Università e della Ricerca Scientifica e Tecnologica, Programmi di Ricerca Scientifica di Rilevante Interesse Nazionale, 2017, [Grant number: 2017FJSM9S]. The authors thank Dr. Liana Cerioni for helpful advice and technical support.

References

- Apostolova, N., Victor, V.M., 2015. Molecular strategies for targeting antioxidants to mitochondria: therapeutic implications. *Antioxid. Redox Signal.* 22, 686-729.
- Bauer, T.M., Murphy, E., 2020. Role of Mitochondrial Calcium and the Permeability Transition Pore in Regulating Cell Death. *Circ. Res.* 126, 280-293.
- Blais, J.D., Chin, K.T., Zito, E., Zhang, Y., Heldman, N., Harding, H.P., Fass, D., Thorpe, C., Ron, D., 2010. A small molecule inhibitor of endoplasmic reticulum oxidation 1 (ERO1) with selectively reversible thiol reactivity. *J. Biol. Chem.* 285, 20993-21003.
- Bonora, M., Patergnani, S., Ramaccini, D., Morciano, G., Pedriali, G., Kahsay, A.E., Bouhamida, E., Giorgi, C., Wieckowski, M.R., Pinton, P., 2020. Physiopathology of the Permeability Transition Pore: Molecular Mechanisms in Human Pathology. *Biomolecules* 10, 998.
- Cantoni, O., Guidarelli, A., 2008. Indirect mechanisms of DNA strand scission by peroxynitrite. *Methods Enzymol.* 440, 111-120.
- Cantoni, O., Guidarelli, A., Fiorani, M., 2018. Mitochondrial Uptake and Accumulation of Vitamin C: What Can We Learn from Cell Culture Studies? *Antioxid. Redox Signal.* 29, 1502-1515.
- Fiorani, M., Azzolini, C., Cerioni, L., Scotti, M., Guidarelli, A., Ciacci, C., Cantoni, O., 2015. The mitochondrial transporter of ascorbic acid functions with high affinity in the presence of low millimolar concentrations of sodium and in the absence of calcium and magnesium. *Biochim. Biophys. Acta* 1848, 1393-1401.
- Flora, S.J., 2011. Arsenic-induced oxidative stress and its reversibility. *Free Radic. Biol. Med.* 51, 257-281.
- Ghezzi, P., Jaquet, V., Marcucci, F., Schmidt, H., 2017. The oxidative stress theory of disease: levels of evidence and epistemological aspects. *Br. J. Pharmacol.* 174, 1784-1796.
- Guidarelli, A., Catalani, A., Spina, A., Varone, E., Fumagalli, S., Zito, E., Fiorani, M., Cantoni, O., 2021. Functional organization of the endoplasmic reticulum dictates the susceptibility of target

cells to arsenite-induced mitochondrial superoxide formation, mitochondrial dysfunction and apoptosis. *Food Chem. Toxicol.* 156, 112523.

Guidarelli, A., Cerioni, L., Fiorani, M., Catalani, A., Cantoni, O., 2020. Arsenite-Induced Mitochondrial Superoxide Formation: Time and Concentration Requirements for the Effects of the Metalloid on the Endoplasmic Reticulum and Mitochondria. *J. Pharmacol. Exp. Ther.* 373, 62-71.

Guidarelli, A., Cerioni, L., Tommasini, I., Fiorani, M., Brune, B., Cantoni, O., 2005. Role of Bcl-2 in the arachidonate-mediated survival signaling preventing mitochondrial permeability transition-dependent U937 cell necrosis induced by peroxynitrite. *Free Radic. Biol. Med.* 39, 1638-1649.

Guidarelli, A., Fiorani, M., Azzolini, C., Cerioni, L., Scotti, M., Cantoni, O., 2015. U937 cell apoptosis induced by arsenite is prevented by low concentrations of mitochondrial ascorbic acid with hardly any effect mediated by the cytosolic fraction of the vitamin. *Biofactors* 41, 101-110.

Guidarelli, A., Fiorani, M., Carloni, S., Cerioni, L., Balduini, W., Cantoni, O., 2016. The study of the mechanism of arsenite toxicity in respiration-deficient cells reveals that NADPH oxidase-derived superoxide promotes the same downstream events mediated by mitochondrial superoxide in respiration-proficient cells. *Toxicol. Appl. Pharmacol.* 307, 35-44.

Guidarelli, A., Fiorani, M., Cerioni, L., Cantoni, O., 2019a. Calcium signals between the ryanodine receptor- and mitochondria critically regulate the effects of arsenite on mitochondrial superoxide formation and on the ensuing survival vs apoptotic signaling. *Redox Biol.* 20, 285-295.

Guidarelli, A., Fiorani, M., Cerioni, L., Cantoni, O., 2019b. The compartmentalised nature of the mechanisms governing superoxide formation and scavenging in cells exposed to arsenite. *Toxicol. Appl. Pharmacol.* 384, 114766.

- Guidarelli, A., Fiorani, M., Cerioni, L., Scotti, M., Cantoni, O., 2017. Arsenite induces DNA damage via mitochondrial ROS and induction of mitochondrial permeability transition. *Biofactors* 43, 673-684.
- Halliday, M., Radford, H., Sekine, Y., Moreno, J., Verity, N., le Quesne, J., Ortori, C.A., Barrett, D.A., Fromont, C., Fischer, P.M., Harding, H.P., Ron, D., Mallucci, G.R., 2015. Partial restoration of protein synthesis rates by the small molecule ISRIB prevents neurodegeneration without pancreatic toxicity. *Cell Death Dis.* 6, e1672.
- Hayes, K.E., Batsomboon, P., Chen, W.C., Johnson, B.D., Becker, A., Eschrich, S., Yang, Y., Robart, A.R., Dudley, G.B., Geldenhuys, W.J., Hazlehurst, L.A., 2019. Inhibition of the FAD containing ER oxidoreductin 1 (Ero1) protein by EN-460 as a strategy for treatment of multiple myeloma. *Bioorg. Med. Chem.* 27, 1479-1488.
- Hosoi, T., Kakimoto, M., Tanaka, K., Nomura, J., Ozawa, K., 2016. Unique pharmacological property of ISRIB in inhibition of A β -induced neuronal cell death. *J. Pharmacol. Sci.* 131, 292-295.
- Hu, Y., Li, J., Lou, B., Wu, R., Wang, G., Lu, C., Wang, H., Pi, J., Xu, Y., 2020. The Role of Reactive Oxygen Species in Arsenic Toxicity. *Biomolecules* 10, 240.
- Jiang, Q., Yin, J., Chen, J., Ma, X., Wu, M., Liu, G., Yao, K., Tan, B., Yin, Y., 2020. Mitochondria-Targeted Antioxidants: A Step towards Disease Treatment. *Oxid. Med. Cell. Longev.* 2020, 8837893.
- Jomova, K., Jenisova, Z., Feszterova, M., Baros, S., Liska, J., Hudecova, D., Rhodes, C.J., Valko, M., 2011. Arsenic: toxicity, oxidative stress and human disease. *J. Appl. Toxicol.* 31, 95-107.
- Kadirvel, R., Sundaram, K., Mani, S., Samuel, S., Elango, N., Panneerselvam, C., 2007. Supplementation of ascorbic acid and alpha-tocopherol prevents arsenic-induced protein oxidation and DNA damage induced by arsenic in rats. *Hum. Exp. Toxicol.* 26, 939-946.
- Koncha, R.R., Ramachandran, G., Sepuri, N.B.V., Ramaiah, K.V.A., 2021. CCCP-induced mitochondrial dysfunction - characterization and analysis of integrated stress response to cellular signaling and homeostasis. *FEBS J.* 288, 5737-5754.

- Minatel, B.C., Sage, A.P., Anderson, C., Hubaux, R., Marshall, E.A., Lam, W.L., Martinez, V.D., 2018. Environmental arsenic exposure: From genetic susceptibility to pathogenesis. *Environ. Int.* 112, 183-197.
- Nurchi, V.M., Djordjevic, A.B., Crisponi, G., Alexander, J., Bjorklund, G., Aaseth, J., 2020. Arsenic Toxicity: Molecular Targets and Therapeutic Agents. *Biomolecules* 10, 231.
- Rabouw, H.H., Langereis, M.A., Anand, A.A., Visser, L.J., de Groot, R.J., Walter, P., van Kuppeveld, F.J.M., 2019. Small molecule ISRIB suppresses the integrated stress response within a defined window of activation. *Proc. Natl. Acad. Sci. USA* 116, 2097-2102.
- Schoof, M., Boone, M., Wang, L., Lawrence, R., Frost, A., Walter, P., 2021. eIF2B conformation and assembly state regulate the integrated stress response. *ELife* 2021, 10, e65703.
- Shen, S., Li, X.F., Cullen, W.R., Weinfeld, M., Le, X.C., 2013. Arsenic binding to proteins. *Chem. Rev.* 113, 7769-7792.
- Sidrauski, C., McGeachy, A.M., Ingolia, N.T., Walter, P., 2015. The small molecule ISRIB reverses the effects of eIF2alpha phosphorylation on translation and stress granule assembly. *ELife* 2015, 4, e05033.
- Sies, H., Jones, D.P., 2020. Reactive oxygen species (ROS) as pleiotropic physiological signalling agents. *Nat. Rev. Mol. Cell Biol.* 21, 363-383.
- Spina, A., Guidarelli, A., Fiorani, M., Varone, E., Catalani, A., Zito, E., Cantoni, O., 2022. Crosstalk between ERO1alpha and ryanodine receptor in arsenite-dependent mitochondrial ROS formation. *Biochem. Pharmacol.* 198, 114973.
- Varone, E., Pozzer, D., Di Modica, S., Chernorudskiy, A., Nogara, L., Baraldo, M., Cinquanta, M., Fumagalli, S., Villar-Quiles, R.N., De Simoni, M.G., Blaauw, B., Ferreiro, A., Zito, E., 2019. SELENON (SEPN1) protects skeletal muscle from saturated fatty acid-induced ER stress and insulin resistance. *Redox Biol.* 24, 101176.

- Vergara-Geronimo, C.A., Leon Del Rio, A., Rodriguez-Dorantes, M., Ostrosky-Wegman, P., Salazar, A.M., 2021. Arsenic-protein interactions as a mechanism of arsenic toxicity. *Toxicol. Appl. Pharmacol.* 431, 115738.
- Wang, F., Zhou, X., Liu, W., Sun, X., Chen, C., Hudson, L.G., Jian Liu, K., 2013. Arsenite-induced ROS/RNS generation causes zinc loss and inhibits the activity of poly(ADP-ribose) polymerase-1. *Free Radic. Biol. Med.* 61, 249-256.
- Wong, Y.L., LeBon, L., Basso, A.M., Kohlhaas, K.L., Nikkel, A.L., Robb, H.M., Donnelly-Roberts, D.L., Prakash, J., Swensen, A.M., Rubinstein, N.D., Krishnan, S., McAllister, F.E., Haste, N.V., O'Brien, J.J., Roy, M., Ireland, A., Frost, J.M., Shi, L., Riedmaier, S., Martin, K., Dart, M.J., Sidrauski, C., 2019. eIF2B activator prevents neurological defects caused by a chronic integrated stress response. *ELife* 2019, 8, e42940.
- Yu, W., Sanders, B. G. and Kline, K. (2003). RRR- α -tocopheryl succinate-induced apoptosis of human breast cancer cells involves Bax translocation to mitochondria. *Cancer Res.* 63, 2483-2491.
- Zyryanova, A.F., Kashiwagi, K., Rato, C., Harding, H.P., Crespillo-Casado, A., Perera, L.A., Sakamoto, A., Nishimoto, M., Yonemochi, M., Shirouzu, M., Ito, T., Ron, D., 2021. ISRIB Blunts the Integrated Stress Response by Allosterically Antagonising the Inhibitory Effect of Phosphorylated eIF2 on eIF2B. *Mol. Cell* 81, 88-103 e106.

Legend to the figures

Fig. 1. ISRIB inhibits ERO1 α expression induced by thapsigargin or arsenite

U937 (A,C) and WT D-C2C12 (B,D) cells were exposed for 6 h to 5 μ M thapsigargin (A,B) or 2.5 μ M arsenite (C,D), in the absence or presence of 200 nM ISRIB, and then analyzed for ERO1 α protein expression. Anti- β -actin antibody was used as a loading control. Results represent the means \pm SD calculated from at three separate experiments. *P < 0.01, as compared to untreated cells. #P < 0.01, as compared to cells treated with thapsigargin or arsenite (ANOVA followed by Dunnett's test).

Fig. 2. ISRIB and EN460 recapitulate the effects of ryanodine on the [Ca²⁺]_c, [Ca²⁺]_m, mitochondrial superoxide formation and DNA damage induced by arsenite

U937, WT D-C2C12 and ERO1 α KO D-C2C12 cells were pretreated for 5 min with the vehicle, 20 μ M Ry, ISRIB or 10 μ M EN460 and incubated for 6 h with the further addition to arsenite. After treatments, the cells were analysed for Fluo 4 (A), Rhod 2 (B) and MitoSOX red (C) fluorescence as well as for DNA damage with the alkaline halo assay (D). In other experiments, cells exposed for 6 h to ISRIB, or EN460, were washed, re-suspended in fresh culture medium, loaded for 20 min with Fluo 4 (E), Rhod 2 (F), or MitoSOX red (G) and subsequently incubated for 10 min with 10 mM Cf and 2.5 μ M arsenite. After treatments, the cells were analyzed for their respective fluorescence responses (E-G) and for DNA damage (H). The results represent the means \pm SD calculated from at least three distinct experiments. *P < 0.05, **P < 0.01, as compared to untreated cells. #P < 0.05, ##P < 0.01, as compared to cells treated with arsenite (ANOVA followed by Dunnett's test).

Fig. 3. The effects of ISRIB or EN460 on U937 and WT D-C2C12 cell viability

U937 and WT D-C2C12 cells were exposed for increasing time intervals to ISRIB, or EN460, and then analysed by counting the number of viable cells (A) and trypan blue positive cells (B). Sister cultures were processed for the assessment of apoptotic chromatin fragmentation/condensation (C). The results represent the means \pm SD calculated from at least three distinct experiments. *P <0.05, **P <0.01, as compared to untreated cells. (ANOVA followed by Dunnett's test).

Fig. 4. Arsenite causes mitochondrial dysfunction and apoptosis *via* mechanisms sensitive to inhibition of the activity or expression of ERO1 α , as well as to its genetic deletion

U937, WT D-C2C12 and ERO1 α KO D-C2C12 cells were pretreated for 5 min with the vehicle, CsA, ISRIB or EN460, and incubated for 16 (A-D) or 24 (E,F) h with arsenite. After treatments, the cells were analysed for MitoTracker red CMXRos-fluorescence (A), MTT reducing activity (B), cytochrome c (Cyt c) immunoreactivity in the cytosolic and mitochondrial fractions (C), cytochrome c localization (D), caspase 3 activity (E), or apoptotic chromatin fragmentation/condensation (F). The results represent the means \pm SD calculated from at least three distinct experiments. *P <0.05, **P <0.01, as compared to untreated cells. #P < 0.05, ##P < 0.01, as compared to cells treated with arsenite (ANOVA followed by Dunnett's test).

Fig. 5. Proposed mechanism whereby EN460 and ISRIB inhibit DNA damage and mitochondrial apoptosis induced by a low concentration of arsenite.

The metalloid promotes an initial activation of the IP₃R, which enhances the expression (sensitive to ISRIB) and activity (sensitive to EN460) of ERO1 α to critically regulate the activation of the RyR. Ca²⁺ release from the RyR (sensitive to Ry⁺) is associated with the mitochondrial accumulation of the cation and with the formation of mitoO₂⁻. Conversion of the latter to H₂O₂ leads to mitochondrial dysfunction and MPT-dependent apoptosis. The diffusible nature of H₂O₂ is also permissive for the

induction of distal effects, as DNA strand scission. Thus, ISRIB and EN460, by preventing the stimulatory effects of ERO1 α on the RyR prevent mitoO₂⁻ formation and its downstream effects leading to DNA strand scission and MPT-dependent apoptosis.

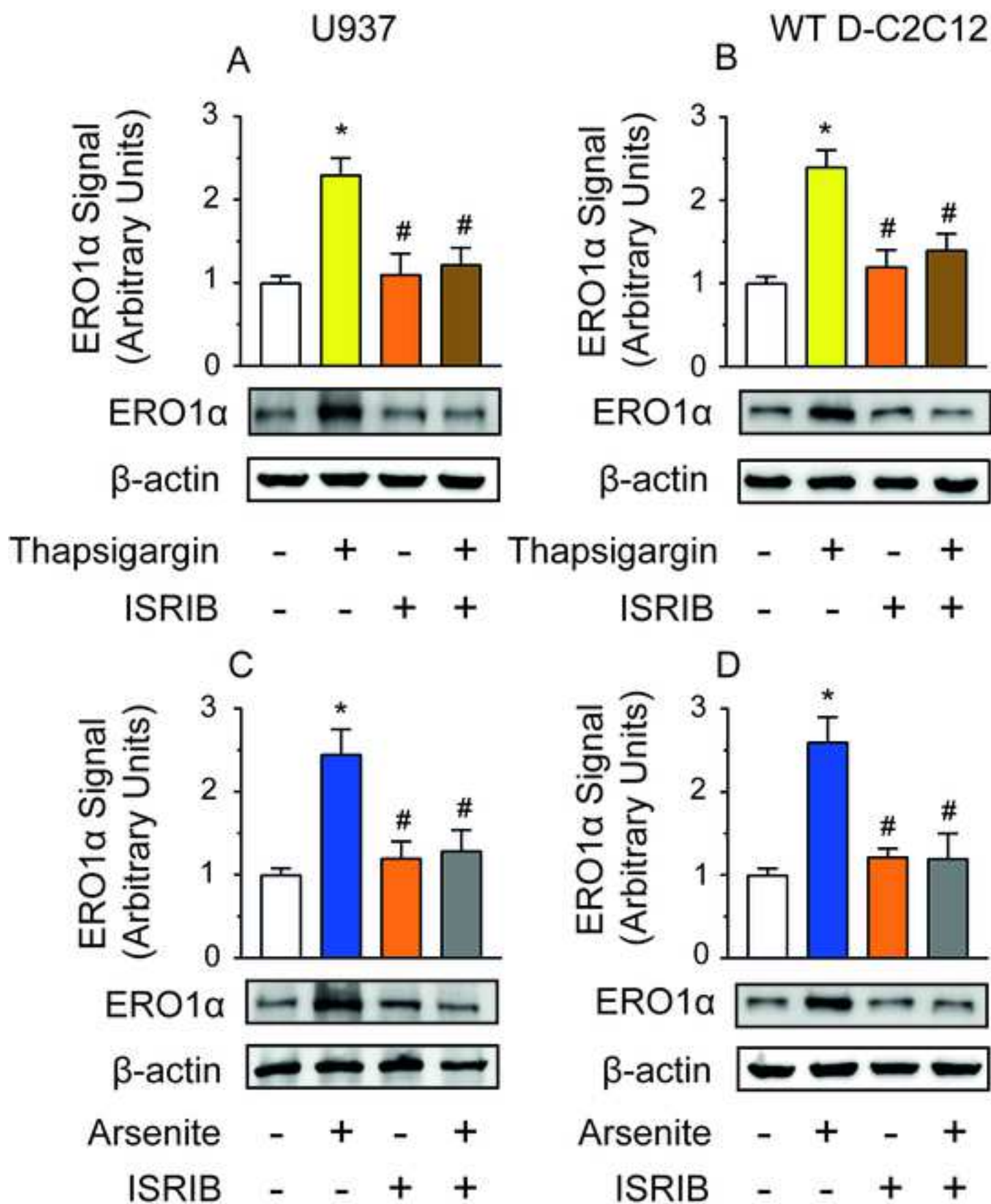


Figure 1

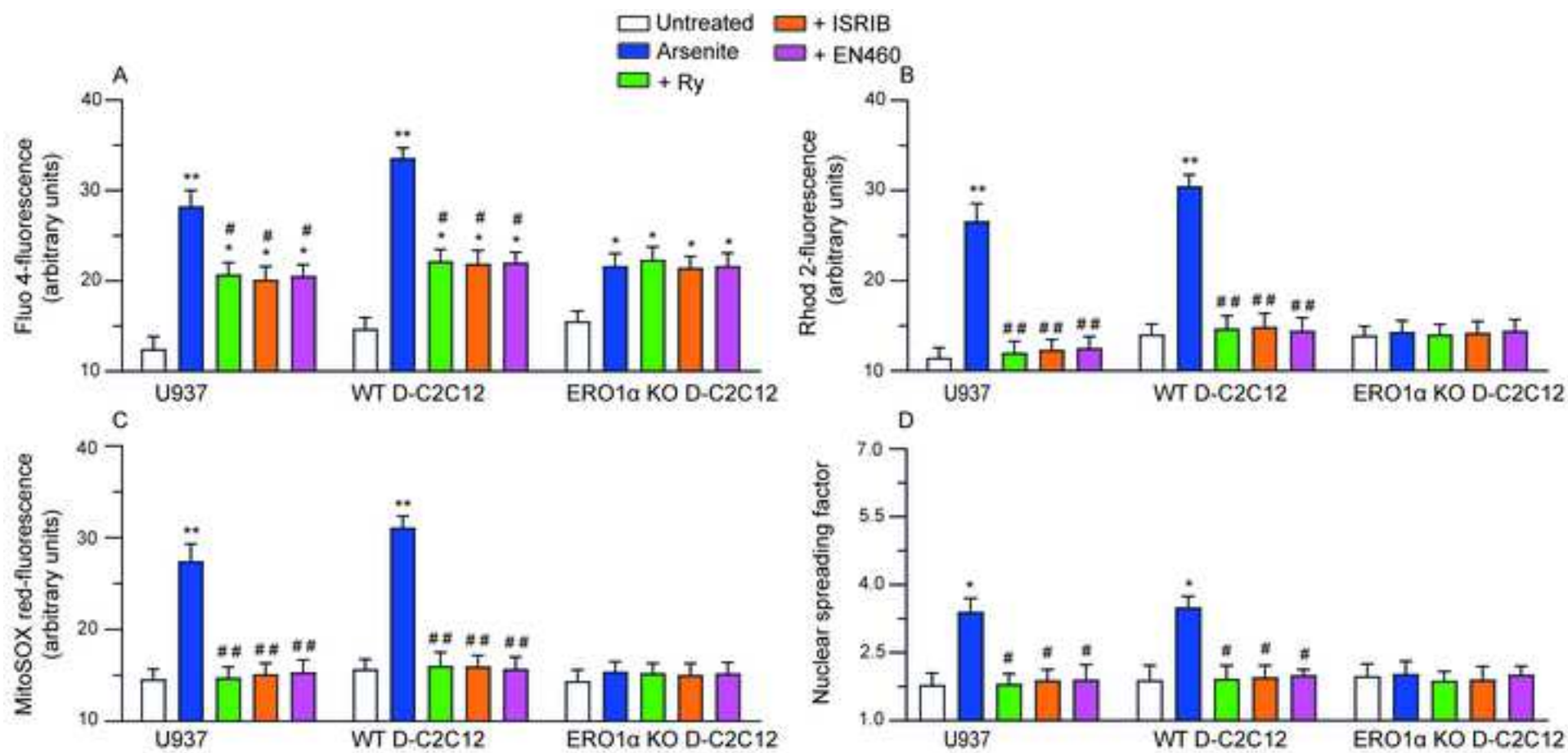


Figure 2

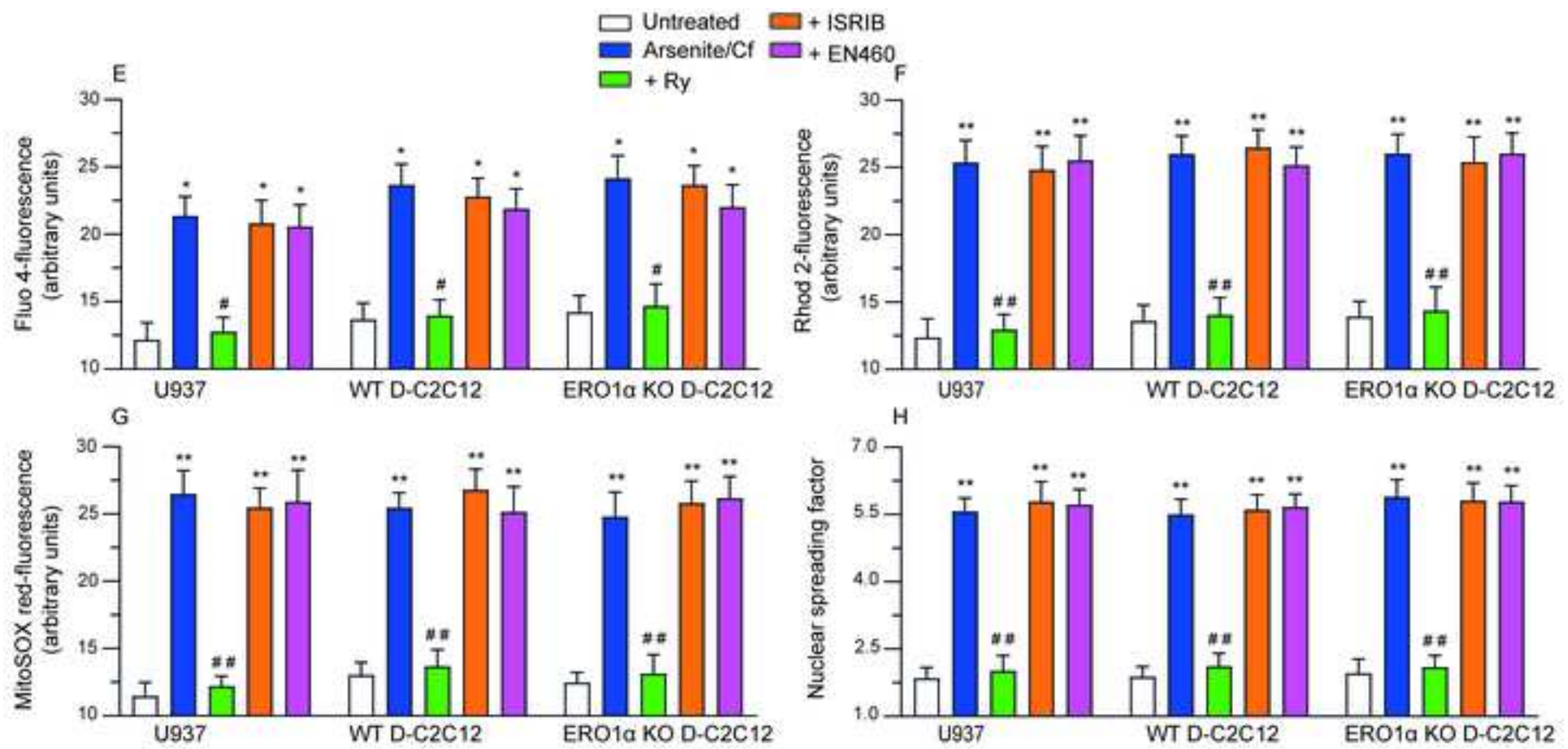


Figure 2 Continued

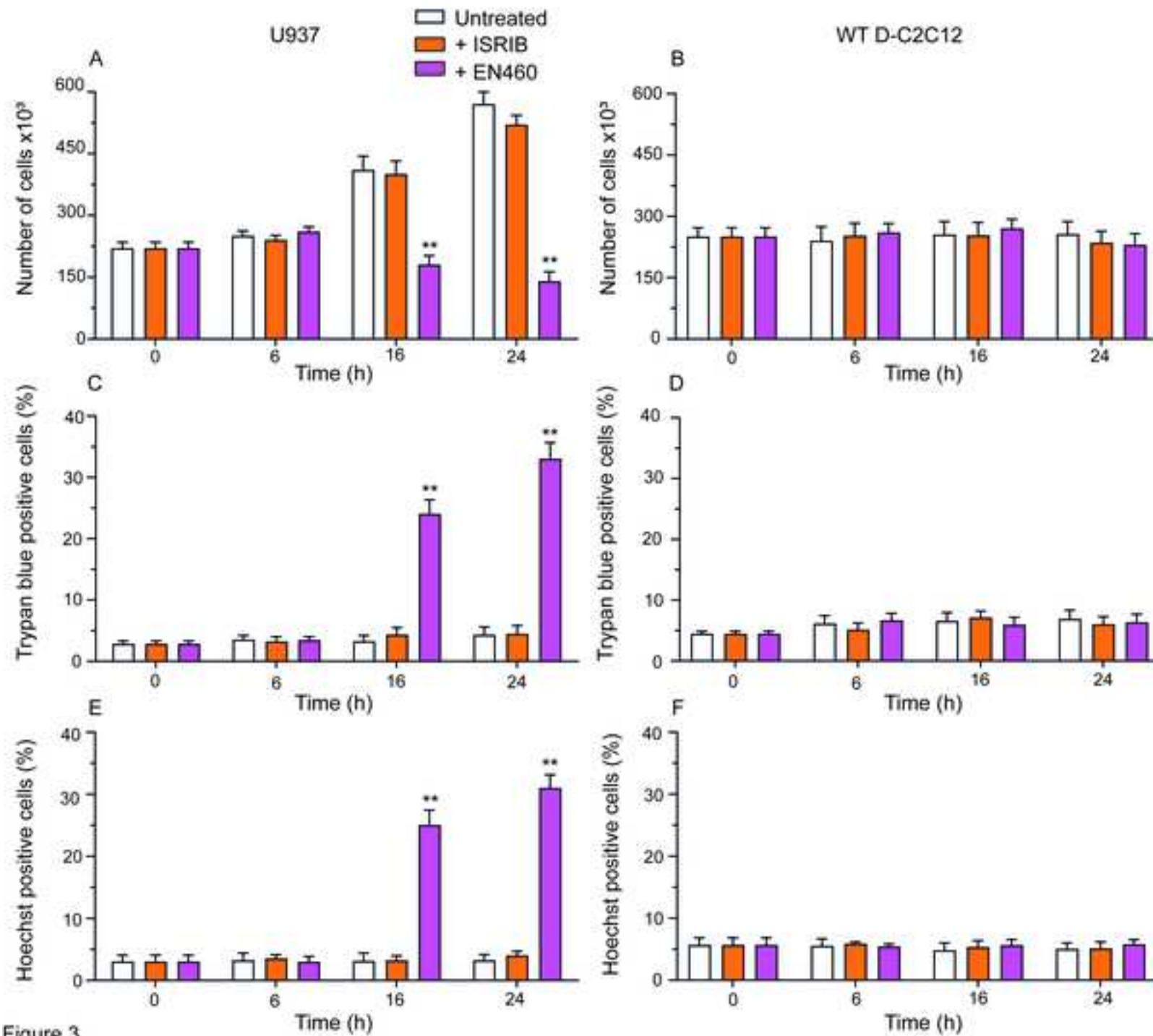


Figure 3

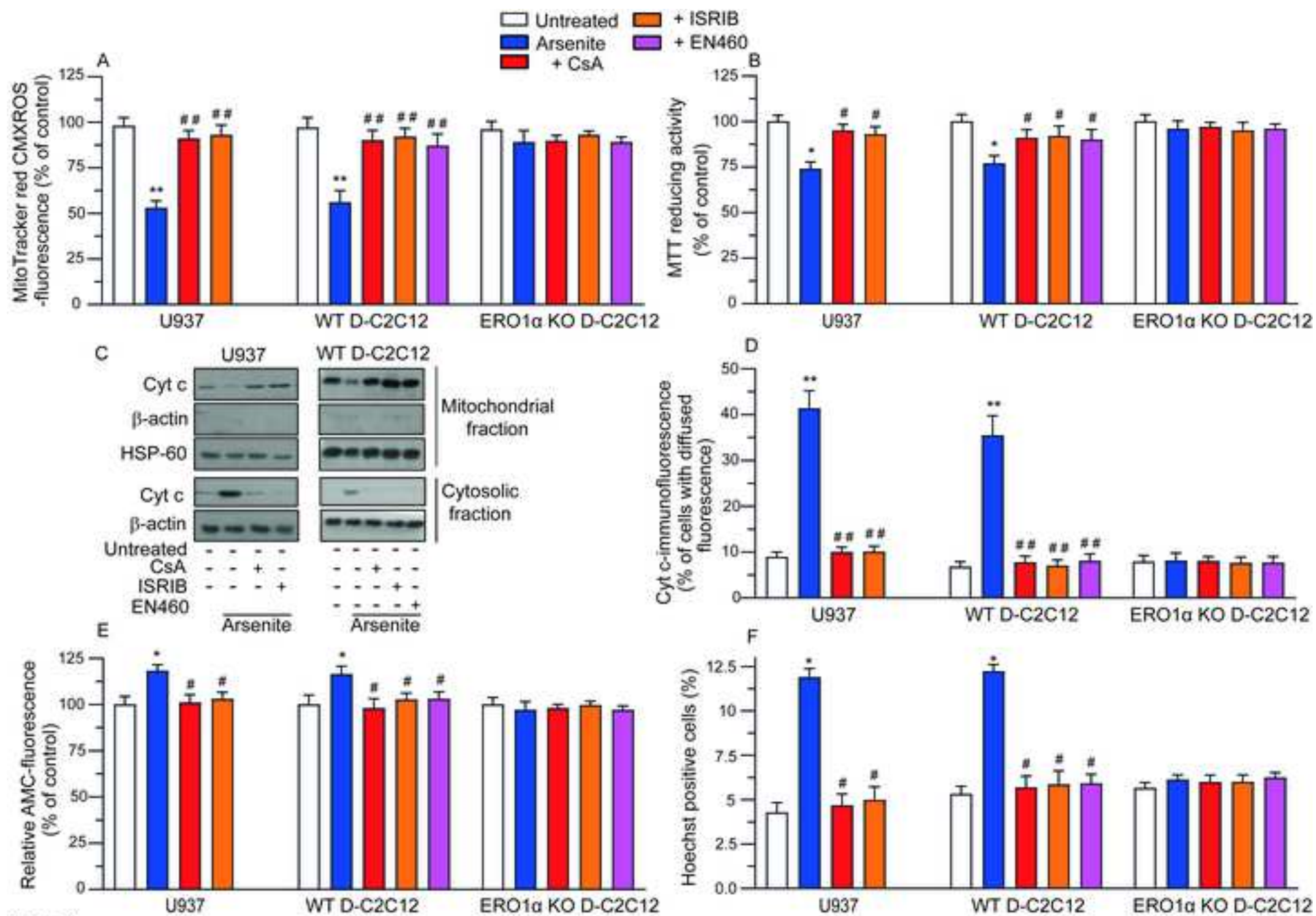


Figure 4

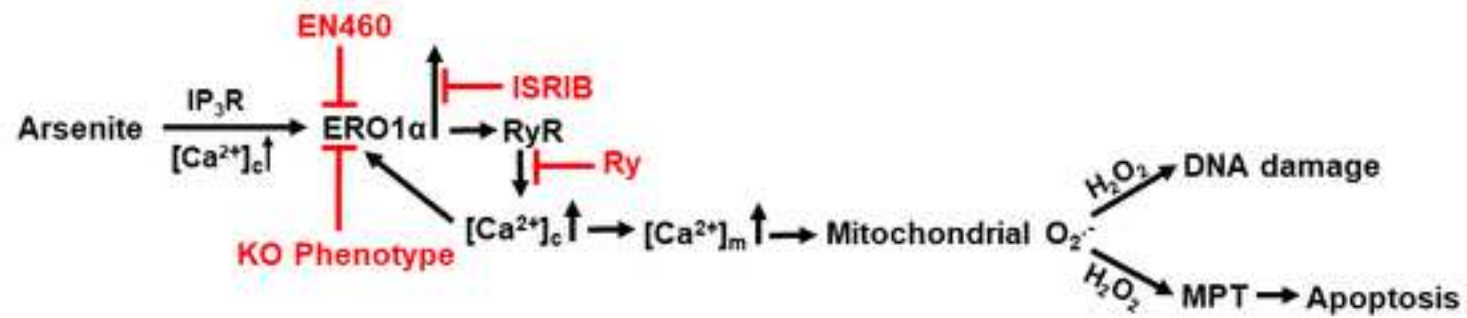


Figure 5

Declaration of interests

The authors declare that they have no known competing financial interests or personal relationships that could have appeared to influence the work reported in this paper.

The authors declare the following financial interests/personal relationships which may be considered as potential competing interests:

CRedit authorship contribution statement

Andrea Guidarelli: Investigation, coordinated the experiments, contributed to the design of the study, data curation, reviewed the manuscript. **Andrea Spina:** Investigation, data curation. **Ester Zito:** Investigation, data curation, reviewed the manuscript. **Mara Fiorani:** Investigation, data curation, reviewed the manuscript. **Orazio Cantoni:** Project administration, contributed to the design of the study, wrote, reviewed and edited the manuscript.